Geochemistry Geophysics Geosystems G3
AN ELECTRONIC JOURNAL OF THE EARTH SCIENCES
Published by AGU and the Geochemical Society

Article
Volume 9, Number 5
21 May 2008
Q05S05, doi:10.1029/2008GC001978
ISSN: 1525-2027

Fluid seepage at the continental margin offshore Costa Rica and southern Nicaragua

Heiko Sahling
Research Centre Ocean Margins, University of Bremen, Klagenfurter Str., D-28359 Bremen, Germany (hsahling@uni-bremen.de)

Formerly at the Sonderforschungsbereich 574, University of Kiel, Wischhofstr 1-3, D-24148 Kiel, Germany

Douglas G. Masson
National Oceanography Centre Southampton, European Way, Southampton SO14 3ZH, UK

César R. Ranero
ICREA at Instituto de Ciencias del Mar, CSIC, Pg. Marítim de la Barceloneta 37-49, E-08003 Barcelona, Spain

Formerly at the Sonderforschungsbereich 574, University of Kiel, Wischhofstr 1-3, D-24148 Kiel, Germany

Veit Hühnerbach
National Oceanography Centre Southampton, European Way, Southampton SO14 3ZH, UK

Wilhelm Weinrebe
Sonderforschungsbereich 574, University of Kiel, Wischhofstr. 1-3, D-24148 Kiel, Germany

Leibniz Institute of Marine Sciences, IFM-GEOMAR, Wischhofstr. 1-3, D-24148 Kiel, Germany

Ingo Klaucke
Leibniz Institute of Marine Sciences, IFM-GEOMAR, Wischhofstr. 1-3, D-24148 Kiel, Germany

Dietmar Bürk
Sonderforschungsbereich 574, University of Kiel, Wischhofstr. 1-3, D-24148 Kiel, Germany

Warner Brückmann
Leibniz Institute of Marine Sciences, IFM-GEOMAR, Wischhofstr. 1-3, D-24148 Kiel, Germany

Formerly at the Sonderforschungsbereich 574, University of Kiel, Wischhofstr 1-3, D-24148 Kiel, Germany

Erwin Suess
Sonderforschungsbereich 574, University of Kiel, Wischhofstr. 1-3, D-24148 Kiel, Germany

Leibniz Institute of Marine Sciences, IFM-GEOMAR, Wischhofstr. 1-3, D-24148 Kiel, Germany

[1] A systematic search for methane-rich fluid seeps at the seafloor was conducted at the Pacific continental margin offshore southern Nicaragua and northern central Costa Rica, a convergent margin characterized by subduction erosion. More than 100 fluid seeps were discovered using a combination of multibeam bathymetry, side-scan sonar imagery, TV-sled observations, and sampling. This corresponds, on average, to a seep site every 4 km along the continental slope. In the northwestern part of the study area, subduction of oceanic crust formed at the East Pacific Rise is characterized by pervasive bending-induced

faulting of the oceanic plate and a relatively uniform morphology of the overriding continental margin. Seepage at this part of the margin typically occurs at approximately cone-shaped mounds 50 - 100 m high and up to 1 km wide at the base. Over 60 such mounds were identified on the 240 km long margin segment. Some normal faults also host localized seepage. In contrast, in the southeast, the 220 km long margin segment overriding the oceanic crust formed at the Cocos-Nazca Spreading Centre has a comparatively more irregular morphology caused mainly by the subduction of ridges and seamounts sitting on the oceanic plate. Over 40 seeps were located on this part of the margin. This margin segment with irregular morphology exhibits diverse seep structures. Seeps are related to landslide scars, seamount-subduction related fractures, mounds, and faults. Several backscatter anomalies in side-scan images are without apparent relief and are probably related to carbonate precipitation. Detected fluid seeps are not evenly distributed across the margin but occur in a roughly margin parallel band centered 28 ± 7 km landward of the trench. This distribution suggests that seeps are possibly fed to fluids rising from the plate boundary along deep-penetrating faults through the upper plate.

Components: 10,061 words, 13 figures, 1 table.

Keywords: chemosynthetic community; authigenic carbonate; subduction erosion.

Index Terms: 3060 Marine Geology and Geophysics: Subduction zone processes (1031, 3613, 8170, 8413); 3004 Marine Geology and Geophysics: Gas and hydrate systems; 3070 Marine Geology and Geophysics: Submarine landslides.

Received 4 February 2008; **Revised** 4 March 2008; **Accepted** 7 March 2008; **Published** 21 May 2008.

Sahling, H., D. G. Masson, C. R. Ranero, V. Hühnerbach, W. Weinrebe, I. Klaucke, D. Bürk, W. Brückmann, and E. Suess (2008), Fluid seepage at the continental margin offshore Costa Rica and southern Nicaragua, *Geochem. Geophys. Geosyst.*, *9*, Q05S05, doi:10.1029/2008GC001978.

1. Introduction

[2] It is generally accepted that fluids play a crucial role at convergent margins, strongly influencing the shallow thermal structure of the downgoing plate, the physical properties of the subduction interface, and the transport of elements to the ocean, the volcanic arc, and the deep mantle. Fluid flow has been intensively studied at accretionary convergent margins, e.g., Nankai [*Le Pichon et al.*, 1992], Cascadia [*Kulm et al.*, 1986], Barbados [*Henry et al.*, 1996], Makran [*von Rad et al.*, 2000] and the Mediterranean Ridge [*Westbrook and Reston*, 2002] whereas margins that are dominated by subduction erosion have received much less attention, even though they make up about 50% of convergent margins worldwide [*Clift and Vannucchi*, 2004; *von Huene and Scholl*, 1991]. The convergent margin offshore Costa Rica and Nicaragua exhibits evidence for subduction erosion, as indicated by long-term, large-scale slope subsidence and associated tectonic extension [*Ranero and von Huene*, 2000; *Ranero et al.*, 2000; *Vannucchi et al.*, 2003].

[3] Fluid flow has been intensively investigated locally in an area offshore the Nicoya Peninsula on the Costa Rican margin during several previous studies (Figure 1). Rapid dewatering of pore water under the outer 3–5 km of the margin wedge, expressed as a decrease in thickness of the underthrust sediments of up to 50%, is indicated by 2-D seismic reflection data [*Shipley and Moore*, 1986]. Further evidence for fluid flow such as a reversed polarity décollement, fault surface reflections and mud mounds were found during a 3-D seismic reflection survey [*McIntosh and Silver*, 1996; *Shipley et al.*, 1990, 1992]. Subsequent *Alvin* dives discovered chemosynthetic communities and authigenic carbonates, which are commonly used as indicators for focused seepage of methane-rich fluids [*Sibuet and Olu*, 1998]. Seepage was found in three structurally distinct areas: at fault scarps on the lower slope, at a mud mound on midslope depths and at strata outcropping at a canyon on the upper slope [*Kahn et al.*, 1996; *McAdoo et al.*, 1996; *Zuleger et al.*, 1996].

[4] Results obtained during Ocean Drilling Program (ODP) Legs 170 and 205 [*Kimura et al.*, 1997; *Morris and Villinger*, 2006] confirmed the seismic evidence for compaction-driven dewatering and revealed evidence for flow systems in two additional structural settings. Compaction of the underthrust ~400 m sediment section in response to loading beneath the margin wedge leads to rapid

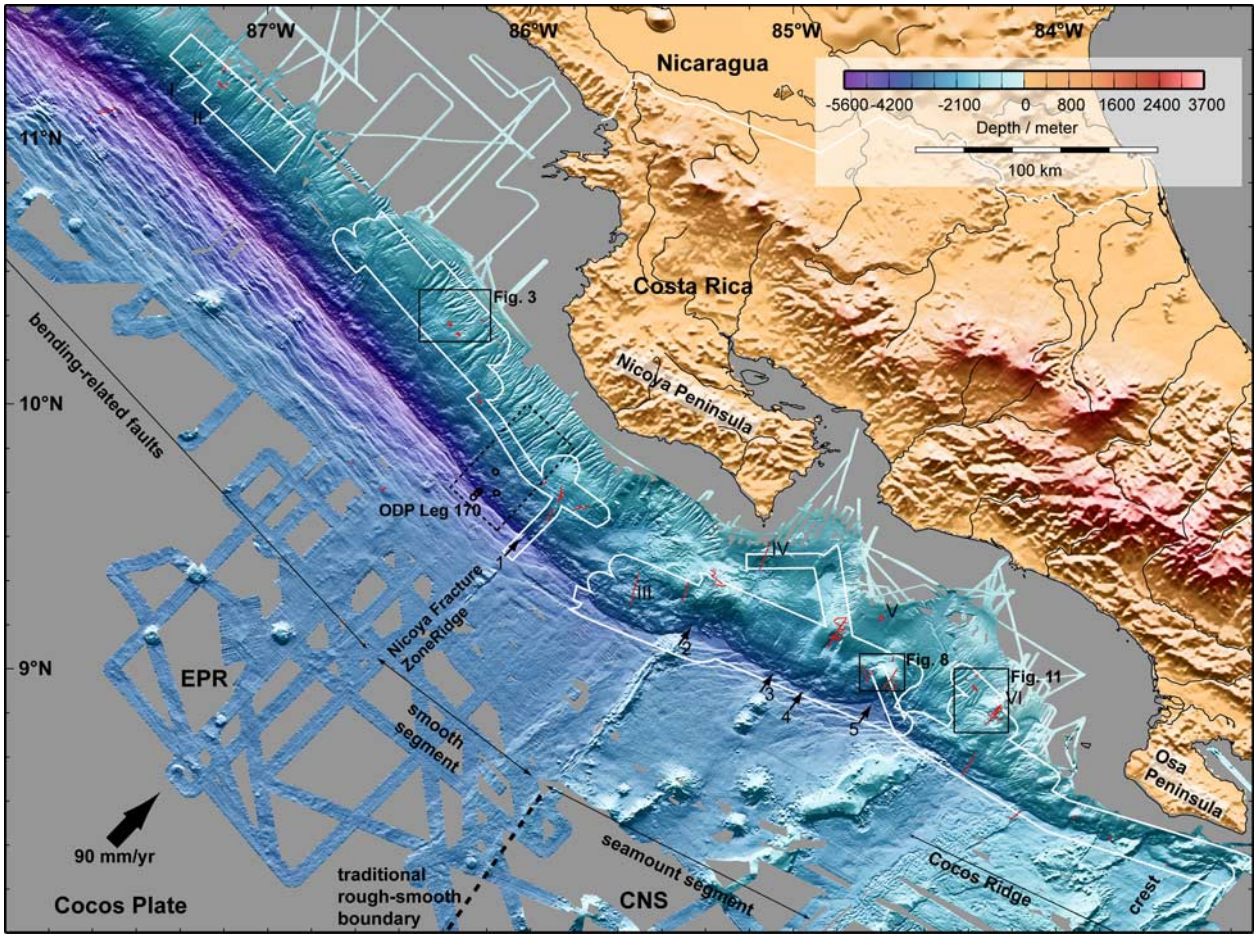

Figure 1. Shaded bathymetry of the continental margin offshore Costa Rica and Nicaragua with the outline of side-scan sonar surveys (white lines) and TV-sled tracks (red lines). Seismic profiling and *Alvin* dives noted in the text were undertaken in the area indicated by the dashed rectangle [*Kahn et al.*, 1996; *McAdoo et al.*, 1996; *Shipley and Moore*, 1986]. In addition, circles designate boreholes drilled during ODP Leg 170 [*Kimura et al.*, 1997] and Leg 205 [*Morris and Villinger*, 2006]. Small black arrows indicate scars caused by seamount and ridge subduction: 1, Fracture Zone Ridge Scar; 2, Rio Bongo Scar; 3, Tarcoles Scar; 4, Jaco Scar; 5, Parita Scar. Roman numbers indicate landslides: I and II, unnamed landslides offshore Nicaragua; III, Nicoya Landslide; IV, Cabo Blanco Landslide; V, BSR Landslide; VI, Quepos Landslide. The locations of Figures 3, 8, and 11 are also shown.

dewatering of pore water within the first 1.5 km of subduction [*Kimura et al.*, 1997; *Silver et al.*, 2000]. Modeling suggests that fluids flow laterally at the top of the underthrust sediments or in the décollement zone [*Saffer et al.*, 2000; *Screaton and Saffer*, 2005] and probably upward through the wedge [*Hensen and Wallmann*, 2005]. In addition, deeply sourced fluids from hydrous mineral dehydration and phase transformation at depths of 10 to 15 km have been identified using geochemical methods. These result in fluid flow both at the décollement and at local faults in the wedge [*Chan and Kastner*, 2000; *Kimura et al.*, 1997; *Silver et al.*, 2000; *Hensen and Wallmann*, 2005].

[5] While the investigations with 3-D seismics, *Alvin*, and ODP focused on a restricted area offshore the Nicoya Peninsula, new discoveries of fluid seeps were made by *Bohrmann et al.* [2002] along a wide segment of the margin offshore central Costa Rica. Chemosynthetic communities were found at a mound, within seamount subduction scars and associated with landslides using TOBI side-scan sonar and video-sled surveys. These findings led the way for the German special program "Sonderforschungsbereich 574" with the overarching objective of investigating the flow of fluids and volatiles in the Middle American subduction complex (http://www.sfb574.uni-kiel.de).

[6] In the frame of this program, we discovered 112 fluid seeps along the margin from offshore southern Nicaragua to south central Costa Rica. This was achieved using a multiscale approach

based on multibeam bathymetry, side-scan sonar imaging and ground-truthing with seafloor observations. Multibeam bathymetry data obtained during various cruises were cleaned and combined to produce a high-resolution seafloor map of the margin (Figure 1). On the basis of these maps, we selected four areas that were surveyed by side-scan sonar systems (Figure 1). Possible fluid flow features identified from backscatter and bathymetry maps were then surveyed during a total of 63 video sled deployments. Subsequently, we integrated individual site observations and extrapolated the pattern to the entire margin in order to identify additional seep-related structures directly from side-scan and bathymetric images. The resulting seep inventory can be sub-divided, according to geological setting, into the following categories: mounds, faults, seamount subduction scars, landslides, and backscatter anomalies without seafloor morphology. Our comprehensive overview of seep structures along the continental margin compliments several detailed studies of individual seeps [e.g., *Linke et al.*, 2005; *Moerz et al.*, 2005; *Mau et al.*, 2006, 2007; *Schmidt et al.*, 2005]. *Han et al.* [2004] showed that almost all of the samples rocks from the seven seep sites are methane-related authigenic carbonates. Furthermore, geophysical studies have been carried out at specific regions, namely offshore southern Nicaragua [*Bürk*, 2007; *Talukder et al.*, 2007], at the slope around Mound Culebra [*Fekete*, 2006; *Grevemeyer et al.*, 2004], at the Hongo mounds offshore the Nicoya Peninsula [*Fekete*, 2006; C. J. Petersen et al., Fluid seepage and mound formation at the Hongo mound field offshore Costa Rica revealed by deep-towed side-scan sonar and subbottom profiler data, submitted to *Geochemistry, Geophysics, Geosystems*, 2008], and at the area of Mound 11 and 12 offshore south central Costa Rica [*Klaucke et al.*, 2008].

[7] A remarkable outcome of this study is that seeping-related structures dominantly occur along a swath at the continental margin at a fairly constant distance landward of the trench. This distribution substantiates the concept of fractured controlled fluid flow related to tectonic processes associated with subduction erosion proposed by *Ranero et al.* [2008] and is in agreement with geochemical evidence for seepage of deeply sourced fluids [*Hensen et al.*, 2004].

2. Study Area

[8] The Cocos Plate offshore Costa Rica and Nicaragua subducts at a rate of about 90 mm a^{-1} below the Caribbean Plate (Figure 1). The relief of the subducting seafloor significantly affects the tectonics, and thus the morphology, of the overriding continental margin. Four distinct oceanic plate segments can be distinguished (Figure 1): (1) The Cocos Ridge is a hot spot ridge formed by the Galapagos hot spot [*Werner et al.*, 1999] with a crest at about 1000 m water depth. Its subduction causes severe deformation of the steep and narrow slope offshore Osa Peninsula [*von Huene et al.*, 2000]. (2) The seamount segment, characterized by many large seamounts and ridges on the oceanic plate, was formed at the Cocos Nazca spreading center (CNS) and later affected by hot spot volcanism. The overriding slope has been indented by at least four seamounts that are in various stages of subduction [*Ranero and von Huene*, 2000; *von Huene et al.*, 2000] and several landslides have probably been triggered by seamount subduction [*von Huene et al.*, 2004b; *Hühnerbach et al.*, 2005]. Seamount underthrusting initially causes deformation of the slope toe colliding with the leading edge of the seamount, followed by uplift of the upper plate as the seamount as subduction continues. Finally, landsliding occurs at its trailing wake. (3) The smooth segment is characterized by a morphologically smooth oceanic plate, although a scar in the upper plate slope within this zone indicates that a precursor of the Nicoya Fracture Zone Ridge has been subducted [*Barckhausen et al.*, 2001]. The Nicoya Fracture Zone Ridge marks the boundary between seafloor generated at the CNS and at the East Pacific Rise (EPR). (4) Bending-related faults oriented parallel to the trench cut pervasively the EPR oceanic crust. The offsets of these faults increase toward the northwest as the trench deepens and the continental slope steepens [*Ranero et al.*, 2003]. Offshore southern Nicaragua, landslides occur due to steepening by tectonic erosion and perhaps subducting relief [*von Huene et al.*, 2004a; *Ranero et al.*, 2008].

3. Material and Methods

[9] This study is based on data obtained during the following cruises with R/V *Sonne* (SO) and R/V *Meteor* (M): SO144 in 1999 [*Bialas et al.*, 1999], SO163 in 2002 [*Weinrebe and Flüh*, 2002], M54 in 2002 [*Söding et al.*, 2002], and SO173 in 2003 [*Flüh et al.*, 2004]. Swath bathymetry was compiled from these and also several earlier cruises [*Ranero et al.*, 2003]. Deep-towed side-scan sonar surveys were collected during cruises SO144 and

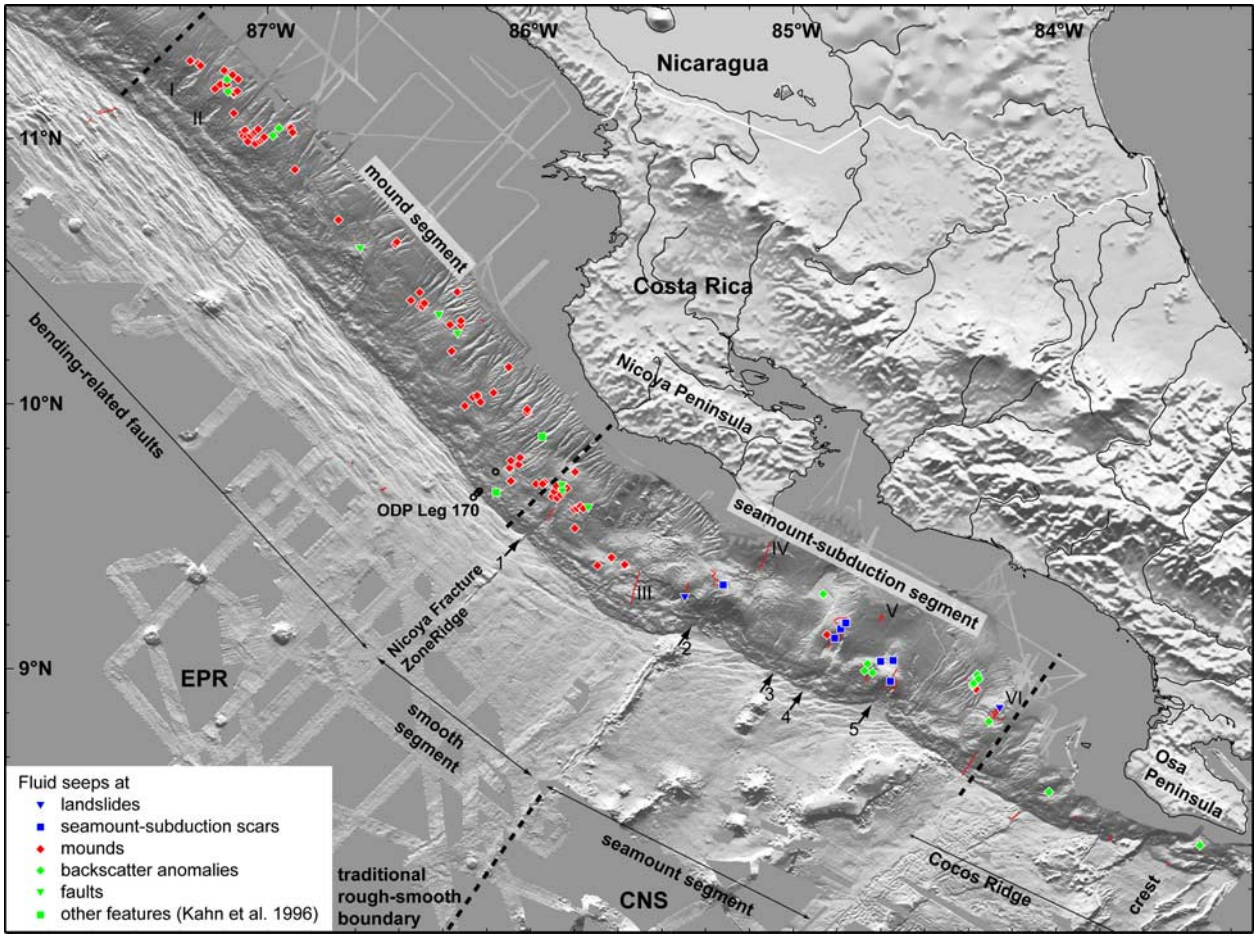

Figure 2. Overview map of locations of 112 methane seeps at the continental margin of Costa Rica and Nicaragua. Different symbols indicate the geological features to which individual fluid seeps are related. The seeps are located along a band at midslope depths. On the basis of the character of seeps we divided the margin into a 240 km long "mound segment" in the northwest and a 220 km long "seamount subduction segment" in the southeast. The margin overriding Cocos Ridge was surveyed by TV-sled tows, but the chaotic background backscatter pattern prevented systematic identification of methane seeps from side-scan data. TV-sled tows (red lines) are shown in order to indicate where searches for seeps were carried out (even if unsuccessful). Numbers are as in Figure 1.

SO163 offshore Costa Rica using the 30-kHz TOBI instrument [*Murton et al.*, 1992], and during cruise SO173 offshore Nicaragua using a 75 kHz Edgetech instrument (DTS-1). TOBI data were processed to a pixel size of 6 m and the higher resolution DTS-1 data to a pixel size of 1 m. Seafloor observations were conducted with ocean floor observation systems (OFOS), TV-sleds provided by R/V *Sonne* (SO163 and SO173) and by the Institut für Geowissenschaften (Kiel, Germany, M54). Both systems were towed behind the ship at about 0.5 knots and 1.5 m above the seafloor, allowing real time observation of a 2 m wide strip of the seafloor along the track. High-resolution 35 mm slides were taken on command by still cameras mounted on the sleds. Some of these images, unfortunately, have a blue-tint due to incorrect white balance. In total 63 TV-sled deployments were made. For completeness, observations made during previous *Alvin* dives [*Kahn et al.*, 1996; *McAdoo et al.*, 1996] have been included in the inventory of seeps (Figure 2 and auxiliary material[1] Table S1).

[10] Working names based on local place names (e.g., Jaco Scar), numbers (Mound 11) or animal names in Spanish (Mound Culebra) were used for all structures investigated in detail. Numbers pre-

[1]Auxiliary materials are available in the HTML. doi:10.1029/2008GC001978

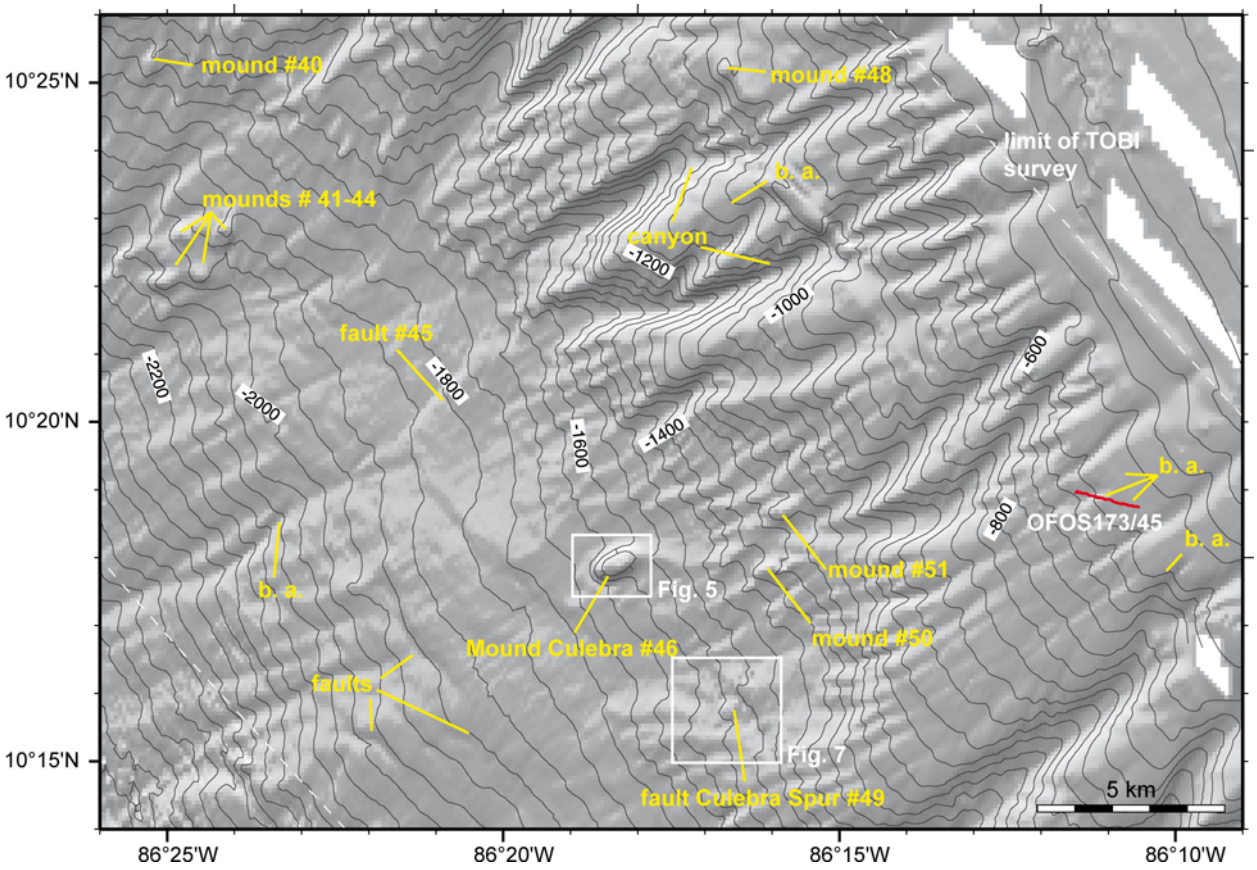

Figure 3. Shaded bathymetric map of the continental slope in the area of Mound Culebra. The major seafloor features identified in the bathymetry as well as in the side-scan sonar image (Figure 4) are canyons at the upper slope at depth between 500 and 1500 m, conical mounds, and faults striking along slope, e.g., fault #45 and fault Culebra Spur (# numbers refer to auxiliary material Table S1). Seafloor observations at Mound Culebra (Figure 5) and fault Culebra Spur (Figure 7) revealed evidence for fluid seepage. In addition, the side-scan sonar image (Figure 4) shows backscatter anomalies (b.a.) that have no seafloor morphology, e.g., at the upper slope. A TV-survey (OFOS173/45) revealed no indications for seeps at these sites.

fixed with a "#" refer to numbers shown in auxiliary material Table S1.

4. Results

[11] Evidence for seepage of methane-rich fluids, such as chemosynthetic communities and authigenic carbonates, was found at 112 sites along some 580 km of continental margin from offshore southern Nicaragua to south central Costa Rica (Figure 2). Seeps were found associated with mounds, faults, seamount subduction scars, and landslides and with backscatter anomalies in the side-scan sonar images where no bathymetric expression could be resolved on multibeam data. The most common findings were numerous roughly conical mounds at the margin offshore southern Nicaragua and northern Costa Rica, where the oceanic bending-related fault segment subducts. The morphology of this margin segment is comparatively uniform. The seamount subduction segment of the margin is, in contrast, morphologically more variable, and sometimes severely deformed by subducting seamounts and ridges. Seepage structures were found to a large extent associated with seamount subduction scars and landslides. The smooth segment forms a transition zone between the bending related fault and seamount subduction zones (Figures 1 and 2). It is included here with the seamount subduction segment for the purposes of reporting the seep inventory, because of the variable morphology of the margin resulting from subduction of the Fracture Zone Ridge and several landslides possibly from past seamount subduction (Figure 2).

[12] Seep-related structures could not be systematically identified on the narrow slope off the Osa

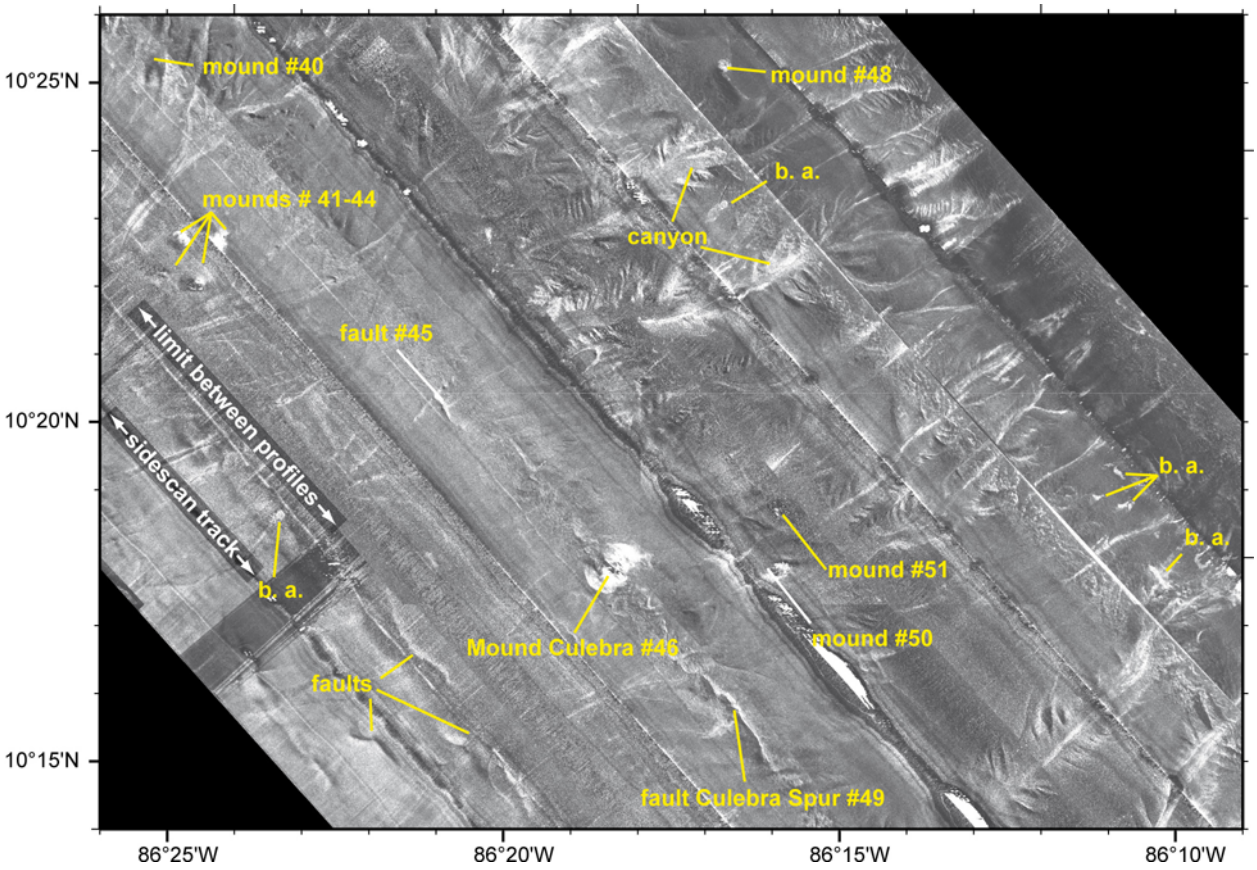

Figure 4. Side-scan sonar image showing the area of the continental slope around Mound Culebra (same area as Figure 3). High backscatter is white; low backscatter is dark. The high-backscatter "fishbone" pattern on the upper slope indicates canyons with feeder channels. Mounds with the steep flanks facing the side-scan fish cause high backscatter, e.g., at mounds #42–44. Flanks that face away from the side-scan have low backscatter, e.g., at mounds #40, 42, and 43. A set of faults with downslope throws strike along the slope northwest and southeast of Mound Culebra. Backscatter anomalies that are not related to positive seafloor structures are marked b.a. (Figure 3).

Peninsula, where we identified only two seep sites despite almost complete mapping of the margin using TOBI side-scan sonar (Figure 1). With the present data we cannot determine whether seep-related seafloor structures are present, or whether they are genuinely absent. Consequently, we do not discuss the results of that segment but concentrate on the mound and seamount subduction segments.

4.1. Seepage at the Mound Segment

4.1.1. Mounds

[13] Sixty mounds were identified from bathymetric and side-scan sonar maps. Most mounds are easily identified because they are cone-shaped or slightly elongated edifices, typically 1 km wide and 50–100 m high. However, they can be more difficult to detect when they occur in areas of rough slope morphology. Steep flanks when crossed in along-slope direction coupled with backscatter anomalies on side-scan sonar images are the key identifying characteristics in this situation.

[14] Twelve mounds were surveyed using the TV-sled. Two additional mounds had also been studied during earlier *Alvin* dives [*McAdoo et al.*, 1996; *Kahn et al.*, 1996]. In summary, 12 of these 14 mounds show evidence for active seepage of methane-rich fluids (auxiliary material Table S1). All show similar characteristics. Authigenic carbonates occur throughout most mound summit areas; chemosynthetic communities are dominated by vesicomyid clam clusters and sporadic occurrences of vestimentiferan tubeworm colonies.

[15] The area around Mound Culebra, nine cone-shaped mounds occur at midslope depths between 900 and 2100 m (Figures 3 and 4). Some mounds,

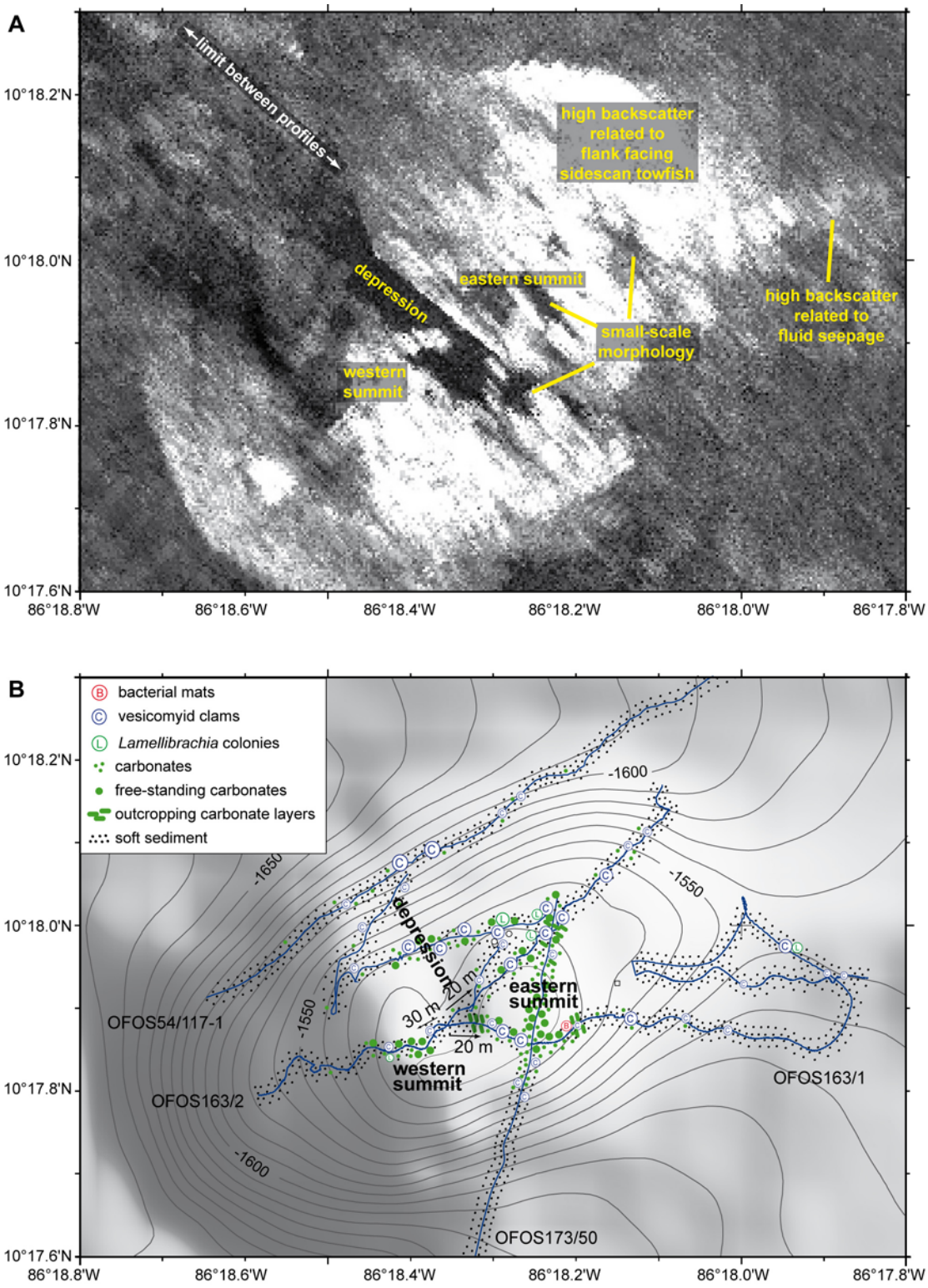

Figure 5. (a) Side-scan sonar image and (b) bathymetry with superimposed seafloor observations at Mound Culebra (modified from *Mau et al.* [2006] with permission from Elsevier). The mound was imaged by two side-scan passes, and as a result, both flanks face the side scan and show high backscatter. The irregular backscatter at the summit and on the northwestern side corresponds to small-scale morphology and the occurrence of authigenic carbonates and chemosynthetic communities revealed by the seafloor observations.

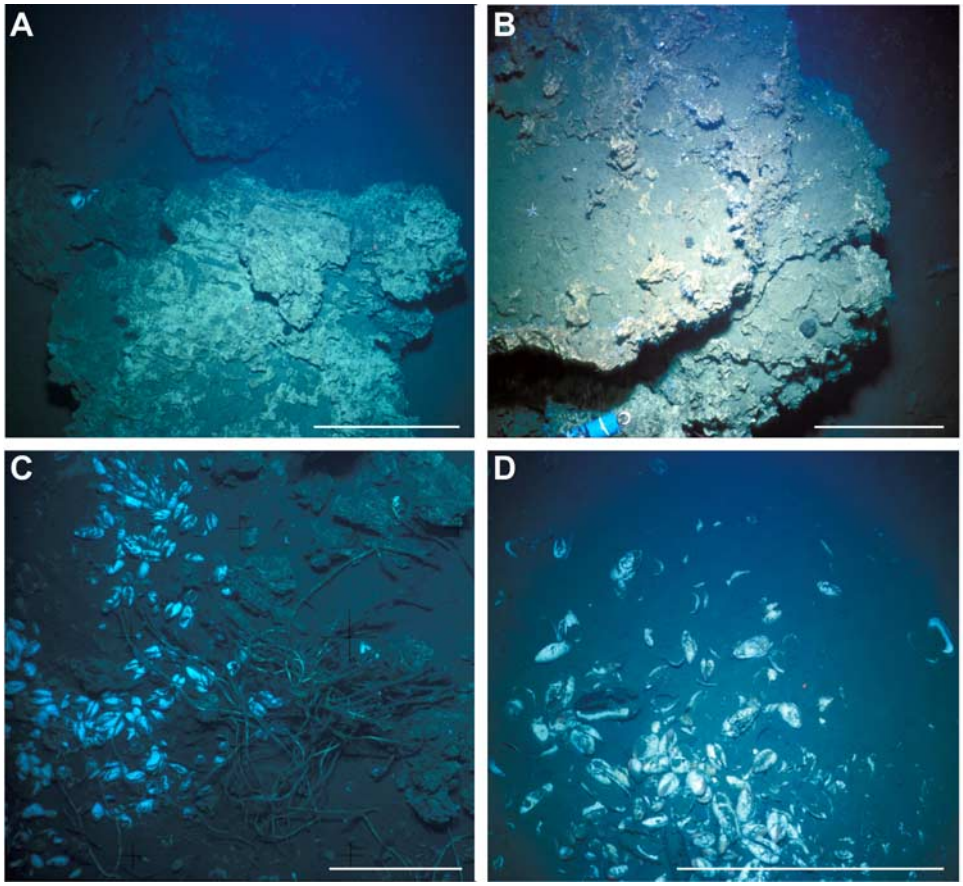

Figure 6. Seafloor pictures taken by TV-sled showing the typical occurrence of authigenic carbonates and chemosynthetic communities at Mound Culebra. (a) Exposed carbonates (M54/117-1, photo: 2_8A). (b) Free-standing large carbonate buildup (M54/117-1, photo: 2_7A). (c) Vesicomyid clam cluster and *Lamellibrachia* colonies surrounded by carbonates (SO163/02, photo: 22:54:50). (d) Clam cluster with living bivalves and shells (M54/117-1, photo: 3_5A). Scale bar 50 cm.

such as Mound Culebra that rises about 140 m above the surrounding seafloor (#46 in auxiliary material Table S1), are clearly visible on the bathymetric map, whereas others are smaller and more difficult to detect in the bathymetry alone (mounds #48, 50, 51). The latter, typically with about 50 m relief, are most easily identified from side-scan images (Figure 4). Some mounds are isolated features, but most mounds occur in clusters (e.g., mounds #41–44).

[16] Extensive seafloor surveys were conducted to calibrate the backscatter patterns at Mound Culebra (Figure 5). High backscatter occurs throughout most of the mound (Figure 5a). Seafloor observations (Figure 5b), however, show that the flanks of the mound are smooth and covered by soft sediments. Most of the high backscatter must consequently be attributed to the steep slopes facing the side scan, or carbonate buried by a thin soft sediment layer. At the summit and the northwestern flank, a linear depression and irregular high and low backscatter pattern indicate small-scale morphology that was confirmed by seafloor observations. Authigenic carbonates forming near-continuous crusts or free-standing edifices a few meters high cover most of the summit (Figures 6a and 6b). These have been sampled and described by *Han et al.* [2004]. Between the carbonates, sediment-filled areas often host vesicomyid clam clusters a few meters in diameter (Figures 6c and 6d). A depression, 20–30 m deep, cuts across the summit area and exposes layers of carbonates. Here, clams and carbonates are less abundant compared to the surrounding summit area. Clam fields, and a few areas hosting vestimentiferan tubeworms and authigenic carbonates occur on the northwestern

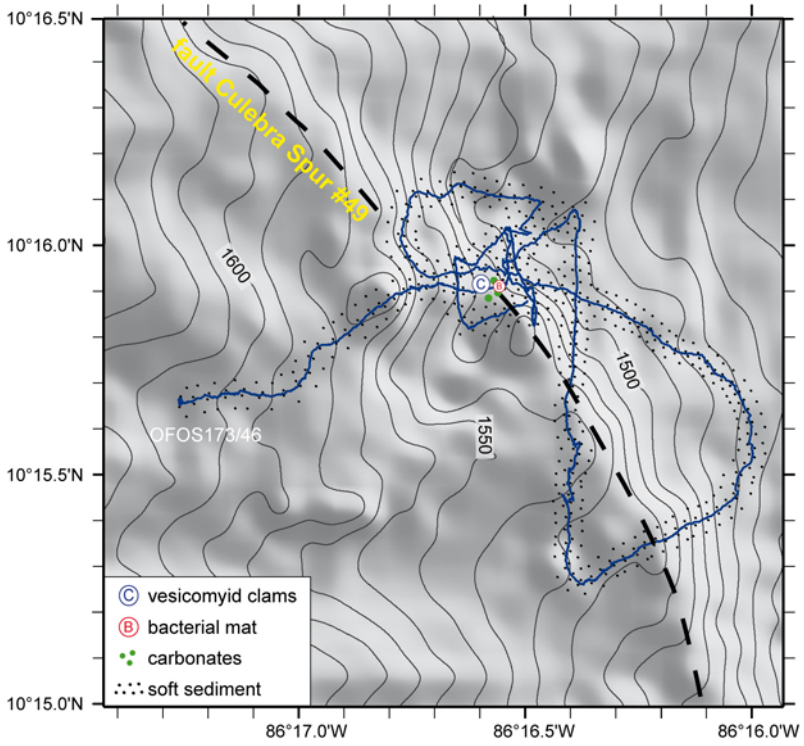

Figure 7. Shaded bathymetry of fault Culebra Spur and the TV-sled survey track. The seafloor surveyed revealed evidence for fluid seepage where the fault is slightly offset. Vesicomyid clams, a patch with bacterial mats, and carbonates were observed in this local area.

flank of Mound Culebra, although carbonates are much less extensive than on the summit.

4.1.2. Faults, Backscatter Anomalies, and Other Seeps

[17] Numerous faults occur across the midslope of the mound segment. Fault Culebra Spur #49 and fault #45, southeast and northwest of Mound Culebra respectively, are typical examples (Figure 4). These faults are most clearly imaged by side-scan sonar, but some can also be traced on the bathymetric map (Figures 3 and 4). A series of TV-sled crossings of the fault scarp of the Culebra Spur Fault revealed restricted occurrences of vesicomyid clams and authigenic carbonates, suggesting that active seepage is focused at discrete points along the linear fault structures (Figure 7). The shaded bathymetry indicates that at this location the fault changes strike slightly and its throw decreases northward, probably indicating that the Culebra Spur fault is composed of a series of linked fault segments.

[18] Numerous other faults along the margin are potential sites of fluid release (Figures 3 and 4). However, the localized character of fault-related seepage means that it is extremely difficult and time consuming to survey these features with the TV-sled. Thus only three faults that show backscatter patterns similar to Culebra Spur are included in the inventory of seep structures (Figure 2 and auxiliary material Table S1).

[19] Several backscatter anomalies without seafloor morphology were imaged by side-scan sonar along the mound segment. We are confident that at least four of these are related to fluid seepage, as they are similar to those backscatter anomalies described in section 4.2.2. They occur in close proximity to mounds (Figure 2 and auxiliary material Table S1) and show backscatter patterns similar to the fluid-seeping-influenced areas of the mounds [*Talukder et al.*, 2007, Figure 3].

[20] On the other hand, several backscatter anomalies without seafloor morphology (Figures 3 and 4) showed only featureless seafloor when surveyed with the TV sled (OFOS173/45). This featureless seafloor may indicate limited fluid seepage that has led to carbonate precipitation at shallow depth within the sediment, which is not observable by

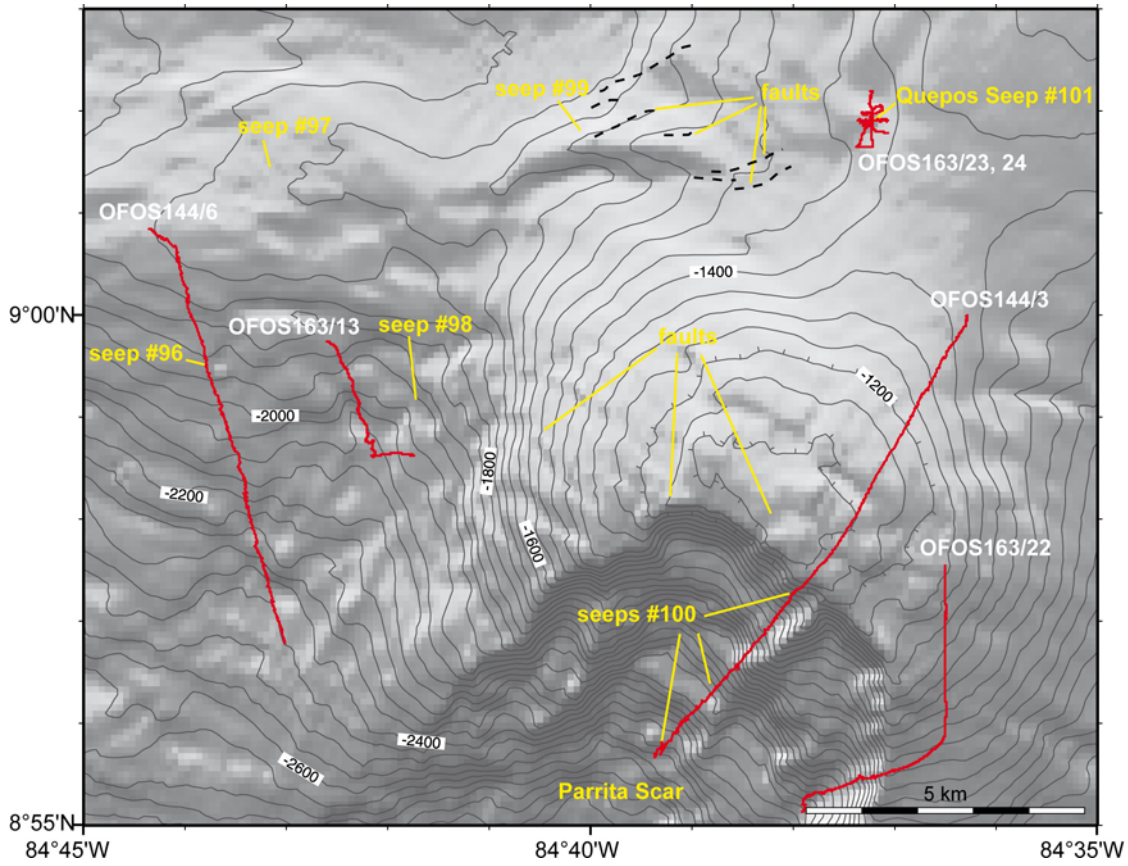

Figure 8. Shaded bathymetry of the Parrita Scar area. The continental margin is uplifted above the subducting seamount, and a scar (depression) is left in its wake due to collapse of the margin behind the subducting seamount. Methane seeps were found in the headwall of the depression and in the landslide debris below it. The locations of backscatter anomalies identified on side-scan sonar data around Parrita Scar (Figure 9) are shown. Several of these have been confirmed as seep sites using TV-sled observations (red lines). Quepos Seep is probably related to faults caused by seamount subduction.

TV-sled, or alternatively to extinct seep features that have become buried by sediments. We excluded them from the list of seep sites (auxiliary material Table S1) due to the lack of clear evidence for currently active fluid seepage.

4.2. Seepage at the Seamount Subduction Segment

4.2.1. Seamount Subduction Scars and Landslides

[21] Seepage related to seamount subduction was studied at Parrita, Jaco and Rio Bongo Scars (numbers 2, 4, and 5 in Figure 2). At these features, seamounts have subducted to different depths beneath the margin and are presently located 20 to 30 km landward of the slope toe. Evidence for methane seepage was found at all three scars but the manifestations vary considerably between them. In general, seepage occurs in three settings related to the deformation process associated with seamount subduction: (1) at the deformed margin landward of the seamount, (2) at the fractured bulge above it, and (3) seaward of the bulge where the margin collapses. Landsliding is an important control on seepage in the last setting. Seepage occurs where permeable strata are exposed in landslide headwalls or fluids that are released from the collapsed landslide mass.

[22] The impact of seamount subduction on the continental margin is illustrated by the example of Parrita Scar (Figures 8 and 9). Here, the continental margin above the subducted seamount is uplifted some 700 m above the surrounding area, causing extensive normal faulting across the bulge (Figure 9). TV-sled surveys revealed fault scarps up to 20 m high characterized by outcropping bedded sediments, but with no evidence for methane seepage.

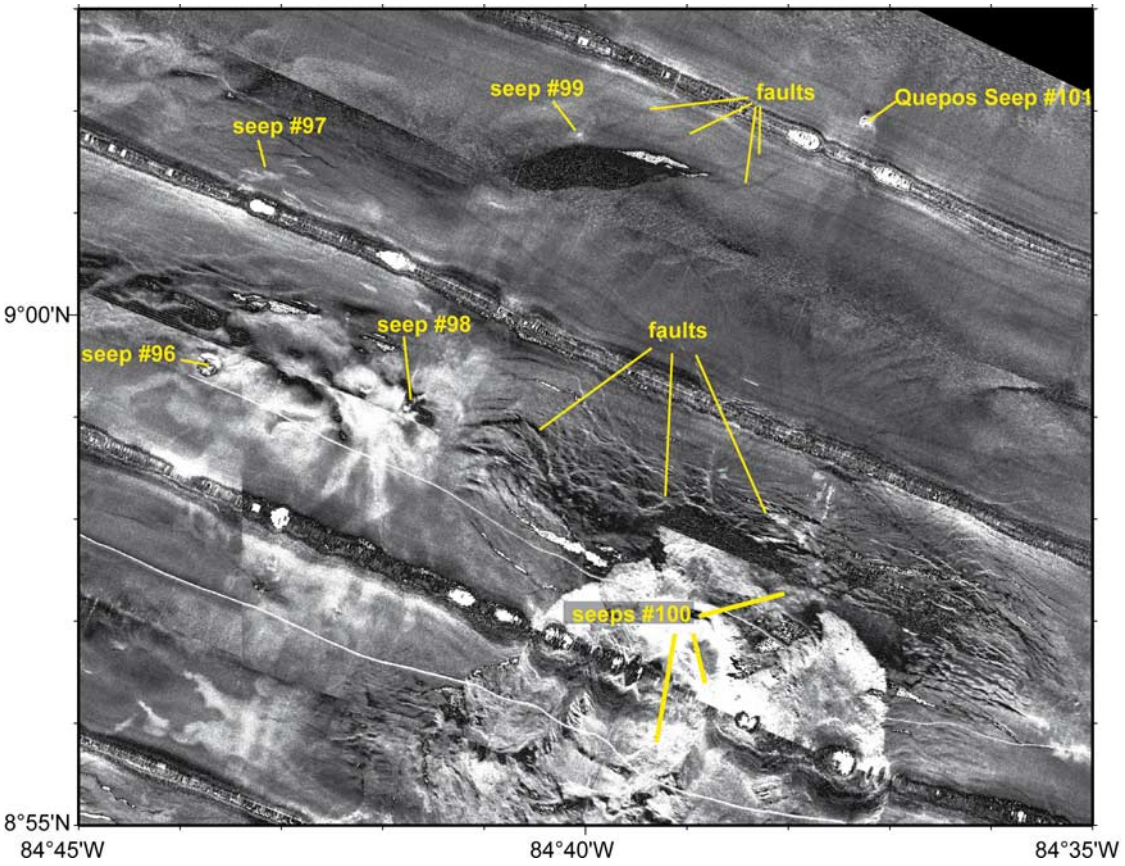

Figure 9. Side-scan image of the Parrita scar area (same area as Figure 8). The uplifted margin above the subducting seamount is extensively faulted. A chaotic pattern of mainly high backscatter characterizes the scar headwall and slide debris. Small irregular backscatter anomalies occur within larger areas with high backscatter west of Parrita Scar. Extensive chemosynthetic communities and authigenic carbonates were observed and sampled at Quepos Seep (Figure 10).

A pronounced headwall marks the limit of mass wasting processes seaward of the seamount. Areas affected by mass wasting are characterized by a complex pattern of high and low backscatter. Chemosynthetic communities (vesicomyid clams, bacterial mats, vestimentiferan tubeworms) were found in small (~1 m across) clusters at three depth intervals (Figures 8 and 9).

[23] Faults and backscatter anomalies, which may indicate fracturing related to uplift ahead of the subducting seamount, also occur landward of Parrita Scar. Two seeps characterized by high backscatter (#99 and Quepos Seep #101; Figures 8 and 9) are associated with an east-west ridge cut by west-southwest trending faults with downslope throw. Quepos Seep is marked by a small circular backscatter anomaly coincident with a ~30 m high ridge. TV-sled data reveal three west-southwest trending ridges, each several meters high, occurring within an area of 250 m in diameter. Seepage is concentrated on the seaward facing ridge slopes where bedded sediments crop out. Extensive fields of authigenic carbonates [*Han et al.*, 2004], vesicomyid clams, mytilid mussels and vestimentiferan tubeworms (*Lamellibrachia barhami* [*McMullin et al.*, 2003]) were found here (Figures 10a and 10b). Quepos Seep is probably fault-controlled, since it is located on a direct extension of one of the west-southwest trending faults (imaged <1 km away) and is marked by ridges with the same trend (Figure 8). This is in contrast to a previous interpretation as a mound (Mound Quepos of *Hensen et al.* [2004]).

[24] The manifestation of seepage and the extent of chemosynthetic communities vary greatly between seamount-subduction scars. At Jaco Scar (number 4 in Figure 2), extensive chemosynthetic communities with dense forests of vestimentiferan tubeworms and clam and mussel beds were found at the lower landslide headwall and in the talus just

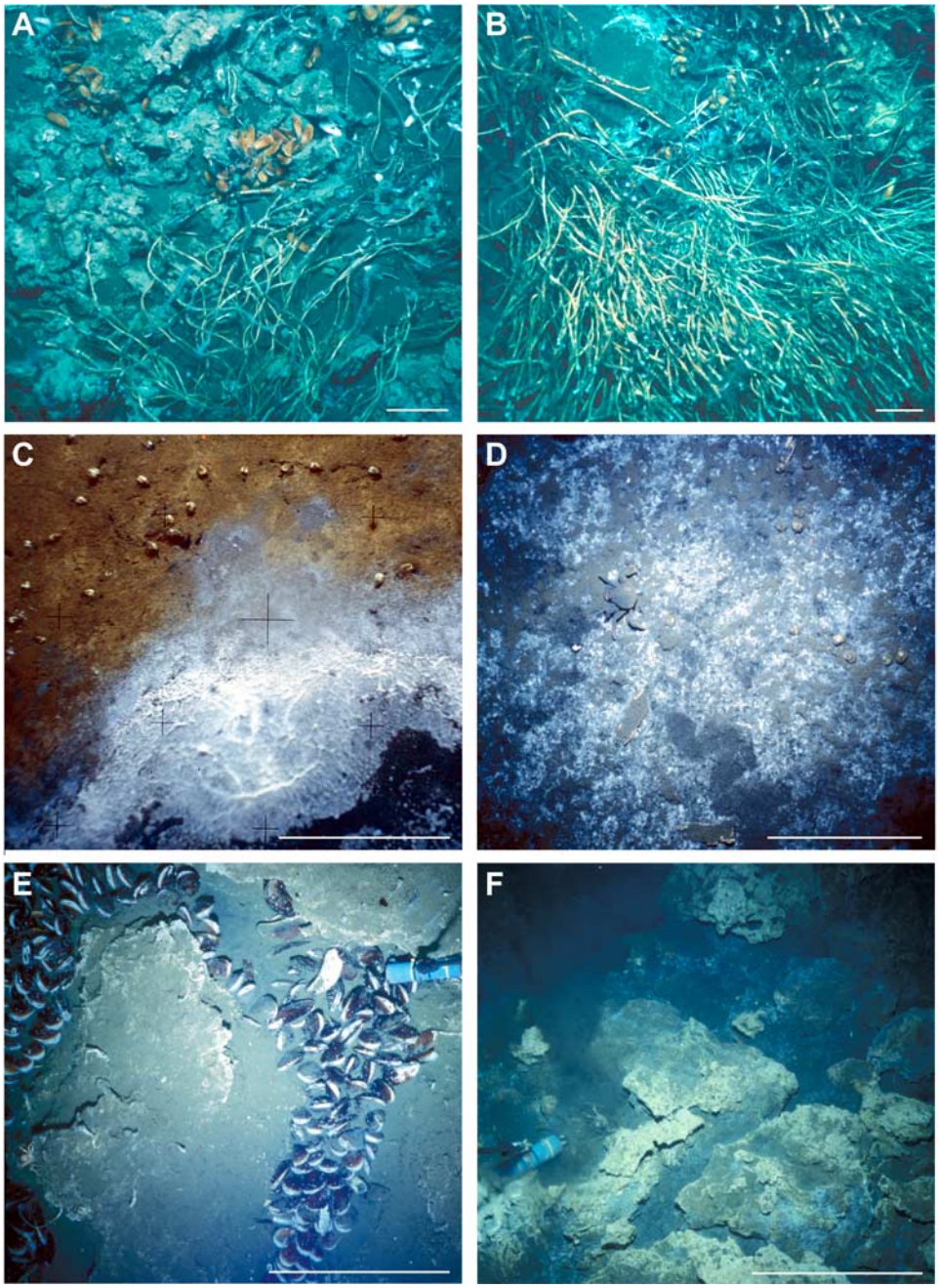

Figure 10. Seafloor pictures taken by the TV-sled at (a and b) Quepos Seep, (c) Quepos Slide, and (d–f) Mound 12. (a) Mytilid bivalves on carbonates (OFOS163/23, photo: 07:16:20). (b) Extensive *Lamellibrachia* colonies (OFOS163/24, photo: 16:25:10). (c) A blackish barren area surrounded by bacterial mats and probably bivalves (OFOS144/4, photo: 08:25:34). (d) Bacterial mats covering a mélange of sediments, carbonates, and shells. Note the sediment-covered decapod (OFOS54/161, photo: 6_29). (e) Mytilid bivalves in cracks of massive authigenic carbonates (OFOS54/161, photo: 5_14). (f) Massive authigenic carbonates (OFOS54/161, photo: 9_7). Scale bar 50 cm.

below. In addition, clam fields were observed at the uplifted seafloor bulge above the seamount. At Rio Bongo (number 2 in Figure 2) an indication for seepage was found at the bulge above the seamount, where a rock platform more than two km wide covers the uplifted seafloor. Here, white bacteria-like mats were observed in cracks between the rocks. Although no sampling was done these

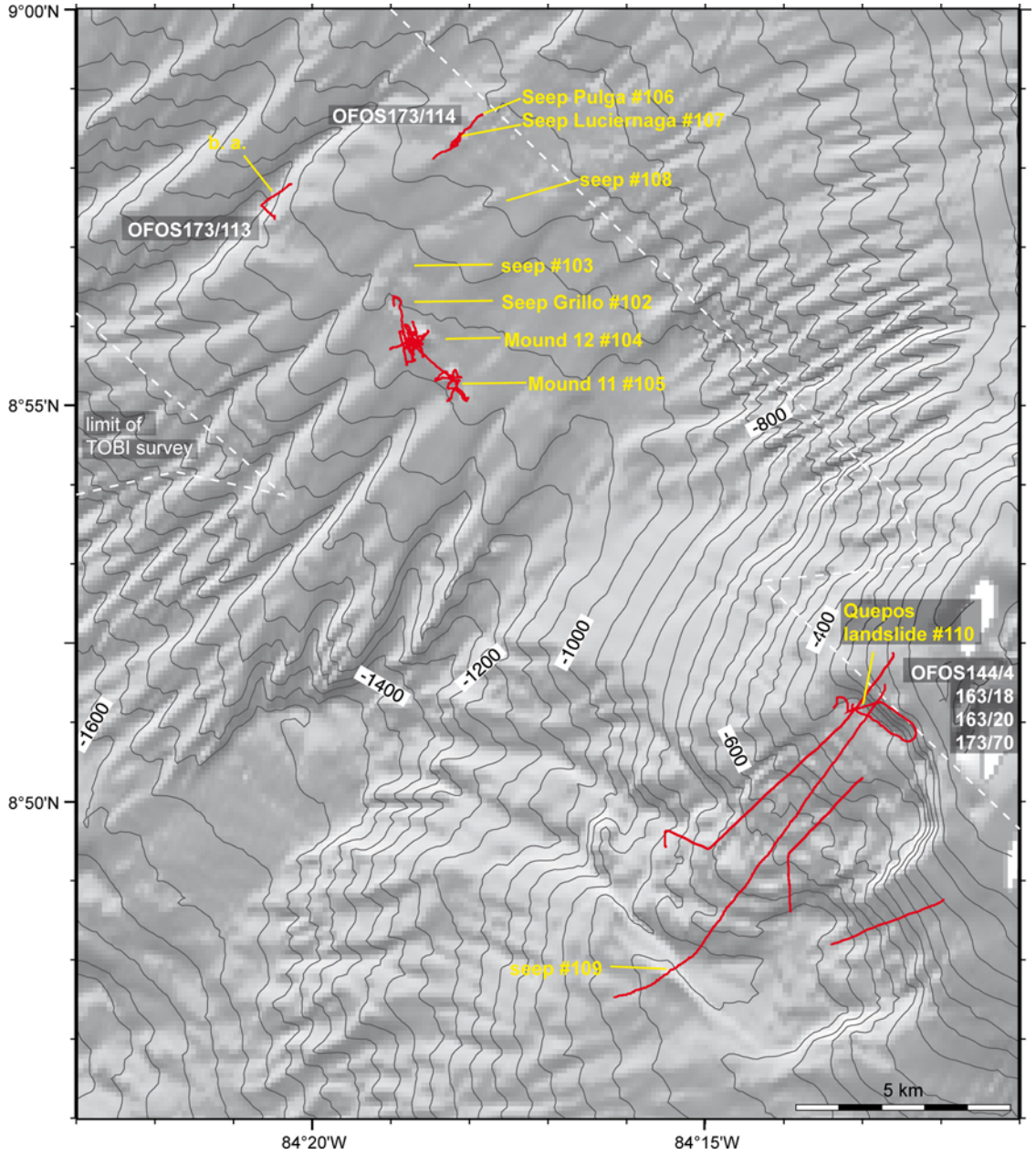

Figure 11. Shaded bathymetry of the Mound 11 and 12 area and Quepos landslide. Fluid seeps were found at Mounds 11 and 12 and the seeps Grillo, Pulga, and Luciernaga, which show backscatter anomalies (Figure 12) but no seafloor morphology. The continental margin above and below these sites is structured by canyons. Large areas are covered with bacterial mats just below the headwall of Quepos landslide (Figure 10c). Red lines show TV-sled survey tracks.

appear to be similar to the bacterial mats observed at, e.g., Mound 11 and 12 that are related to seepage of methane-rich fluids [*Hensen et al.*, 2004].

[25] Evidence for seepage was found at two of the four landslides at the seamount subduction segment (III-VI in Figure 2). Chemosynthetic communities are most extensive at Quepos landslides, which influenced a 10-km wide area of the slope (Figures 11 and 12). Bacterial mats covering an area of tens of m^2 on top of very soft sediments immediately below the headwall at depths of around 400 m were imaged by TV-sled surveys (Figure 10c). The backscatter at this site is low, in contrast to the high backscatter encountered at all

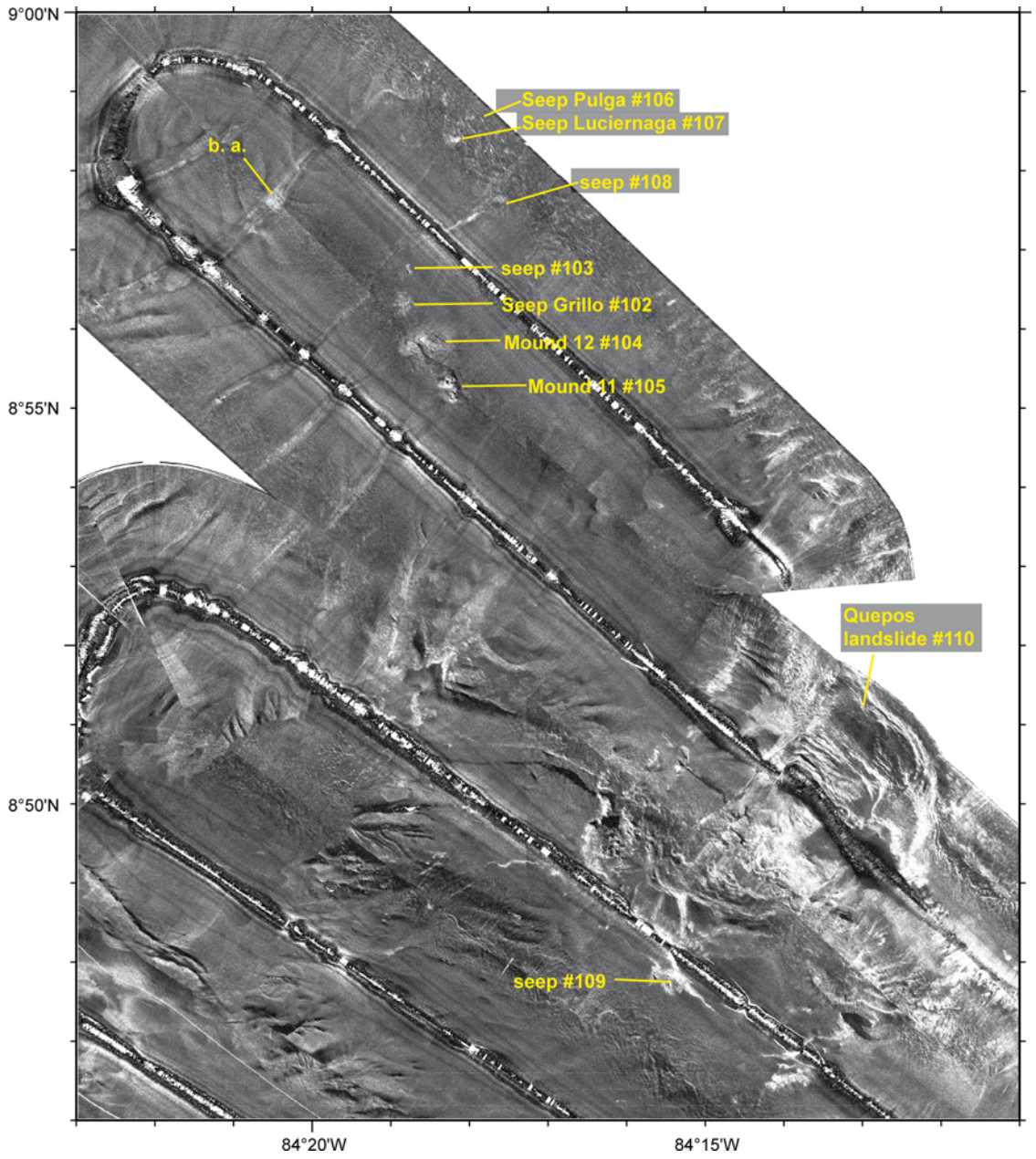

Figure 12. Side-scan sonar image of the Mound 11 and 12 area and Quepos landslide (same area as Figure 11). Fluid seeps were found at several backscatter anomalies without seafloor morphology. TV-sled survey of the backscatter anomaly (b.a.; see also Figure 11) at the canyon axis northwest of the mounds revealed exposed hard substrate but no evidence of seepage.

other seeps. It is in agreement, however, with bottom sampling that recovered very soft but gas-rich sediments and only a small piece of authigenic carbonate [*Han et al.*, 2004].

4.2.2. Mounds, Faults, and Backscatter Anomalies

[26] The manifestation of seepage related to mounds, faults and backscatter anomalies is more complex at the seamount subduction segment than at the mound segment, as illustrated by the two following examples.

[27] Near the southeastern end of the seamount subduction segment, several mounds and backscatter anomalies are located at water depths of 850 to 1050 m in an area of smooth slope with a relatively gentle slope gradient. This smooth area separates steeper areas on the upper and middle slopes that

Table 1. Summary of Numbers of Fluid Seeps Associated With Various Seafloor Structures Along the Continental Margin Segments Offshore Southern Nicaragua and Costa Rica[a]

	Margin Width, km	Mounds	Backscatter Anomalies	Faults	Other	Landslides and Seamount Subduction	Total
"Mound segment"	240	60	4	3	2		69
"Seamount subduction segment"	220	17	11	3		1 seep at Quepos slide 1 seeps at Nicoya slides 1 seep at Rio Bongo Scar 4 seeps at Jaco Scar 3 seeps at Parrita Scar	41
Margin overriding Cocos Ridge	120		2				2
Total	580	77	17	6	2	10	112

[a] The seeps at the lower and upper slope described by [*Kahn et al.*, 1996; *McAdoo et al.*, 1996] are denoted as "other."

are incised by canyons (Figures 11 and 12). The mounds and seeps (#102–105) are oriented nearly parallel to the slope along a NNW-SSE lineament. Mounds 11 and 12 are up to 1000 m across and have high backscatter and 30 m of seafloor relief [*Klaucke et al.*, 2008] whereas Seep Grillo #102 and seep #103 are smaller and characterized by high backscatter without relief. The proximity of the various mounds and backscatter anomalies, and their alignment along a single lineament suggest seepage related to a common process, despite the variability of their expression in seabed morphology.

[28] TV-sled tows (Figure 11) reveal evidence for fluid seepage in the form of bacterial mats, clams and authigenic carbonates at all these features. The main difference between no-relief seeps and mounds is that the area displaying seepage-related manifestations is larger at mounds, and the buildup of carbonates is both greater and of more complex structure than at no-relief seeps. For example, video sled observations at Mound 12 shown in Figure 6 of *Mau et al.* [2006] reveal that this mound is characterized by a successive occurrence of a mélange of shell fragments and carbonate pieces in sediments (Figure 10d), fractured carbonates with mytilid bivalves (Figures 10e and 10f), and massive carbonates. This pattern is probably a result of increasing carbonate precipitation with time. Comparison of TV-sled observations with the backscatter maps shows that the outcrop of carbonates at the seafloor can explain most of the high backscatter imaged with TOBI side-scan sonar. However, the area of high backscatter is generally larger than the area of exposed carbonates. Carbonates buried at shallow depth in the sediments are not visible to TV-sled observations, but imaged thanks to the few-tens-cm penetration of side-scan sonar signal account for the wider distribution of high backscatter [*Klaucke et al.*, 2008].

[29] The second example shows the complex nature of backscatter anomalies that occur on the slope west of Parrita Scar (Figures 8 and 9). Here, small irregular high and low backscatter areas occur within a broad area of high backscatter (Figure 9). Two TV-sled surveys (Figure 8) showed that soft sediments covered the entire area but a few scattered clam shells were found. We suggest the complex high and low backscatter patterns relate to fluid seeps (#96 and #98) but that these were not detected by TV-sled surveys because their seabed expression is spatially restricted. Furthermore, high backscatter may indicate diffuse seepage producing cementation of shallow sediments, detectable with side-scan sonar, but not recognized by TV-sled observations.

[30] Numerous backscatter anomalies without seafloor morphology occur at the seamount subduction segment (Figures 8–9 and 11–12). However, we included only eleven of these, where TV-sled evidence of seepage exists or the morphology on side-scan sonar images suggest active seepage, in our list of seep sites (Table 1 and auxiliary material Table S1). This careful approach probably results in a conservative estimate of seep numbers. Direct evidence for seepage, in the form of massive authigenic carbonates, bacterial mats or scattered clamshells was found at five of the eleven backscatter anomalies. Additional systematic sampling is needed to confirm to what extent high backscatter at these sites is related to occurrence of authigenic carbonates at and/or immediately below the seabed.

[31] The 17 mounds discovered in the seamount subduction segment generally differ in morphology and their manifestation of seepage from those

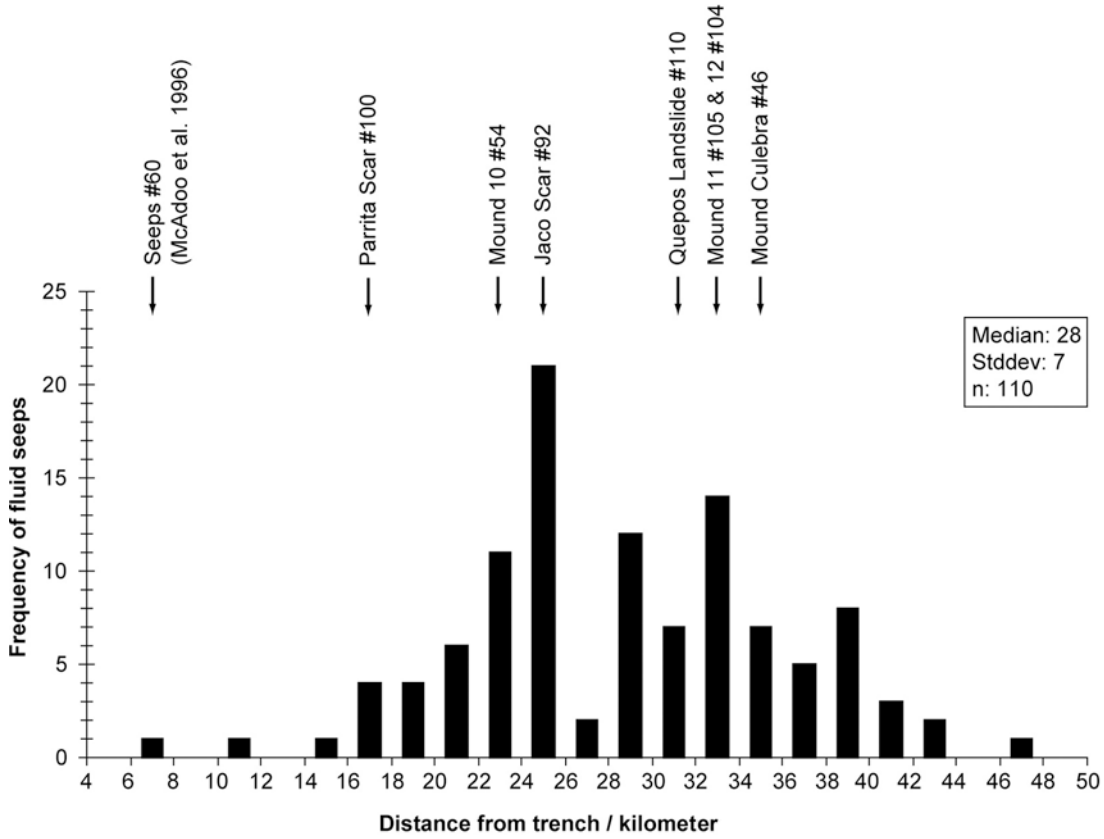

Figure 13. Frequency of fluid seeps on the slope plotted against distance from the trench. To simplify the distance measurements, the reentrants in the deformation front caused by seamount subduction were neglected and a straight margin was assumed.

relatively uniform mounds in the mound segment. In the seamount subduction segment, mound morphology varies considerably between features, it is often complex and relatively subdued, the small-scale morphology is structured by authigenic carbonates, and the composition of chemosynthetic communities is more variable.

4.3. Distribution of Fluid Seeps

[32] The results of the systematic search for fluid seeps at the seafloor along the Costa Rican and Nicaraguan margins are summarized in Figure 2. Seeps occur in a margin-parallel swath at a relatively constant distance landward of the trench (Figure 13). The Gaussian-type frequency distribution shows that 90 % of the seeps are located 17–40 km behind the trench (Figure 13).

5. Discussion

[33] The multiscale approach used in this study, combining swath-bathymetry, side-scan sonar and TV-sled data, revealed the presence of a minimum of 112 seeps along the ~580 km long continental margin from offshore southern Nicaragua to southern Costa Rica (Figure 2). While mounds are the dominant seep-related feature at the mound segment, features associated with seepage at the seamount subduction segment are diverse and include seamount subduction scars, landslides, mounds, faults and backscatter anomalies without seafloor morphology.

5.1. Seepage at the Mound Segment

[34] A total of 69 seeps were identified at the 240 km long mound segment. The most intriguing seep-related features are the 60 mounds that are remarkably similar in size, shape and in the occurrence of authigenic carbonates as well as chemosynthetic communities (e.g., Mound Culebra; Figures 3–6). Authigenic carbonates or chemosynthetic communities were found at twelve of the fourteen mounds examined using the TV-sled, so it is reasonable to infer that most of 60 mounds identified are actively seeping methane-rich fluids.

[35] However, our understanding of how these mounds evolve is still fragmentary. High-resolution seismic reflection data show that Mound Culebra is related to a normal fault [*Fekete*, 2006] and it seems likely that many mounds are fault controlled. They are formed by the extrusion of highly viscous sediments leading to the cone-shape morphology with very steep flanks [*Moerz et al.*, 2005]. No evidence for flows of low-viscosity mud have been found in side-scan sonar images nor is there any for mud breccias in sediment cores [*Moerz et al.*, 2005]. The ubiquitous presence of authigenic carbonates at the summit areas of the mounds suggests a long seepage history but there are no data to estimate their ages.

[36] In general, fluid flow at the mounds is low in comparison to other submarine mud volcanoes. This low fluid flow rate is indicated by the composition of chemosynthetic communities at the mounds. Vesicomyid clams are associated with lower fluxes of chemical compounds than, for example, bacterial mats [*Mau et al.*, 2006]. Furthermore, direct flux estimates based on modeling of chemical gradients suggests flow rates in the order of 0.1 to 2 cm a^{-1} [*Ranero et al.*, 2008]. These values are low compared to values in the range of 8 to 250 cm a^{-1} obtained at the mud volcanoes Dvurechenskii in the Black Sea [*Wallmann et al.*, 2006], Atalante and Cyclops offshore Barbados [*Henry et al.*, 1996; *Wallmann et al.*, 2006], and Håkon Mosby off Norway [*De Beer et al.*, 2006]. These mud volcanoes have a flat-toped morphology and show evidence for mudflows indicating water-rich mud expulsion during discrete eruptive phases, which is a contrast to the cone-shaped mounds in our study. The form of the mounds suggests that relatively little water is available during the extrusion of mud forming the cone-shaped morphology.

[37] Seepage at faults is difficult to detect and analyze, because flow occurs at small, localized areas (Figure 7). Because faulting across the slope is pervasive, seepage at faults is likely to be an important process. However, it is not possible to readily detect active seepage on faults on the basis of the available geophysical data. Thus, despite the widespread presence of faults at the mound segment, only three fault segments are included in the inventory of setif (Table 1 and Figure 2). This is almost certainly a highly conservative estimate of seep abundance. Additional evidence for fluid seepage at faults was obtained during *Alvin* dives at the lower slope offshore the Nicoya Peninsula, where chemosynthetic communities occur at fault scars characterized by high reflection amplitudes in 3-D seismic data [*Kahn et al.*, 1996; *McAdoo et al.*, 1996; *McIntosh and Silver*, 1996].

5.2. Seepage at the Seamount-Subduction Segment

[38] Subduction of seamounts and ridges causes intense deformation of the overriding plate offshore south central Costa Rica [*Ranero and von Huene*, 2000; *von Huene et al.*, 2000, 2004b; *Hühnerbach et al.*, 2005]. Here 41 fluid seepage sites were found along a 220 km long segment. Seeps are related to a variety of structures including landslides, seamount subduction scars, mounds, faults and backscatter anomalies. The diversity of seeps found at this segment differs from the uniformity of cone-shaped mounds at the mound segment. While an estimate of total fluid seepage at the mound segment is feasible, such an order-of-magnitude calculation is more difficult for the seamount-subduction segment due to the diversity of seep structures. Furthermore, estimating the extent of seepage at features such as seamount subduction scars and landslides is difficult due to the size and complexity of these features. For example, landsliding at the trailing edge of the seamount at Parrita Scar has an impact on an 8 km wide stretch of the slope (Figure 9). In this area, it is practically unfeasible to differentiate backscatter anomalies related to fluid seepage from the overall complex pattern of high and low backscatter caused by the rough topography. Thus, we do not know the extent of each seep beyond the restricted areas surveyed during TV-sled tows.

[39] Mound 11 and 12 and nearby backscatter anomalies, located in the southeast of the seamount-subduction segment, illustrate the diversity of seep-related features at this margin segment (Figures 11 and 12). The diversity of mounds (and other seep structures) precludes a generalization of a seep type at this margin segment. We stress this fact as it is tempting to generalize individual results obtained at a selected feature [*Hensen et al.*, 2004, *Mau et al.*, 2006]. For example, Mound 11 and 12 are unusual in many respects. First, fluid fluxes expressed as Darcy flux at a location of Mound 11 are the highest measured at the continental margin offshore Costa Rica with values up to 3 m a^{-1} [*Hensen et al.*, 2004]. A high rate of supply of reduced chemical compounds, indicated by the chemosynthetic communities that are dominated by bacterial mats and mytilid

bivalves [*Mau et al.*, 2006], also suggests that fluid fluxes are comparatively active at both mounds 11 and 12. Second, benthic fluxes are high in sediments covered by bacterial mats at Mound 12 [*Linke et al.*, 2005]. Third, gas hydrates and methane of a primarily thermogenic origin were uniquely recovered at Mound 11 [*Schmidt et al.*, 2005].

[40] *Klaucke et al.* [2008] compared TOBI and DTS-1 side-scan sonar as well as sediment echosounder data and published seafloor observations at Mounds 11 and 12 [*Mau et al.*, 2006]. They proposed that these features have probably been formed by a process different from that which formed the cone-shaped mounds at the mound segment. There is no evidence for extensive mudflows as proposed before [*Moerz et al.*, 2005] and most of the backscatter patterns can be explained by carbonate distribution. The authors concluded that the subdued morphology and differences in the reflectivity pattern of the features are most likely the result of differential burial by mass wasting deposits and continental slope erosion.

5.3. Distribution of Fluid Seeps

[41] The occurrence of seeps in a broad band along the margin 17–40 km landward of the trench (Figures 2 and 13) is consistent with the concept that deep-sourced fluids play a key role in the evolution of the erosive convergent margin [*Ranero et al.*, 2008]. Mineral dewatering at the plate boundary releases water at temperatures in the range of ~50 to ~160°C mainly by the transformation of biogenic opal to quartz and smectite to illite. Hydraulic fracturing by fluids near lithostatic pressures probably causes basal erosion of the upper plate, gradually shifting the plate boundary upward [*von Huene et al.*, 2004a; *Ranero et al.*, 2008]. This basal erosion results in subsidence and extensional faulting of the overriding margin. The fluids percolate through deep-penetrating, high-permeability extensional faults and are expelled at the seafloor on the slope. The compilation of data shown in Figure 2 convincingly argues for a deep source of fluids expelled at the band of seeps along the slope, since most seeps occur above the plate boundary where temperatures are >60 to ~140°C [*Ranero et al.*, 2008].

[42] *Hensen et al.* [2004] showed that the low chlorinity of pore waters recorded at seeps is a result of mineral dewatering reactions at plate boundary depths, confirming the source of the seep fluids. Their study is based on geochemical data from Mound Culebra, Mounds 10, 11, 12 and Quepos Seep (Mound Quepos of *Hensen et al.* [2004]) located 24–35 km landward of the trench, i.e., in the typical seep position (Figure 13).

[43] The band of fluid seeps, located 17–40 km landward of the trench, indicates that this swath is probably the zone where most of the methane-rich fluids are expelled. However, previous studies have also indicated flow of deeply sourced fluid closer to the trench. Deep-sourced fluids were found at ODP Site 1040, located just 1.6 km landward of the trench. Lithium isotopic composition of pore water indicates these fluids result from mineral dewatering reactions at depth that flow seaward along the décollement and escape through faults in the wedge [*Chan and Kastner*, 2000]. Moreover, seeps were found during *Alvin* dives that are located 5–8 km behind the trench, also seaward of the main band of seeps described here [*Kahn et al.*, 1996; *McAdoo et al.*, 1996]. This observation questions the above statement on the distribution of seeps and whether seeps at the lower slope have not been detected with our methodological approach.

[44] However, we argue that, if seepage of methane-rich fluids at the lower slope were a significant process, evidence for this process would have been found using the TV-sled. None of the six deployments at lower slope depths (Figure 2) revealed evidence for seepage. Seeps such as those discovered during *Alvin* dives are thus probably small-scale, spatially limited features and their contribution to the overall flow of methane-rich fluids through the margin is likely to be small compared to the abundant seeps concentrated 17 to 40 km landward of the trench.

[45] We might further question why compaction-driven fluid flow does not lead to the occurrence of typical evidence of seeps, such as chemosynthetic communities or authigenic carbonates, on the lower continental slope close to the trench. It is known that compaction of underthrust sediments leads to rapid dewatering within the first few kilometers of subduction at this margin [*Saffer et al.*, 2000]. Geotechnical measurements and modeling of fluid flow suggest that these fluids flow seaward through the upper sediment sequences or along the décollement. Some fluids may also flow upward influencing the thickness and depths of the gas-hydrate bearing zone [*Hensen and Wallmann*, 2005]. However, neither extensive *Alvin* dives [*Kahn et al.*, 1996; *McAdoo et al.*, 1996] nor TV-sled surveys during several R/V *Sonne* and R/V *Meteor* cruises

revealed any evidence for seepage at the trench axis or through the toe of the overriding plate. The most likely explanation is that the fluids do not contain sufficient methane to support chemosynthetic communities since the methane content of pore water in the compacted sediments is low [*Kimura et al.*, 1997]. As a result, seepage of methane-depleted pore fluids may not be detected by visual observations of the seafloor.

6. Conclusions

[46] A systematic search for evidence of fluid seepage using a combination of multibeam bathymetry, side-scan sonar and seafloor observations has shown that fluid venting is widespread along the continental margin offshore Costa Rica and Nicaragua. We identified 110 seeps along a 460 km long stretch of the continental slope, although this number is considered a minimum estimate. On average, one seep occurs every 4 km along slope, although in practice the distribution of cold seeps is uneven. Seepage of methane-rich fluids is concentrated in the midslope region at a distance of 28 ± 7 km from the trench. Seeps are associated with seafloor mounds or backscatter anomalies on side-scan sonar data. Seep distribution is likely to be related to mineral dewatering processes at the plate boundary that provide fluids that subsequently circulate upward through the margin. Faulting related to subduction erosion and seamount subduction along this margin provides the pathways for these fluids.

[47] Our results, as well as those from other active and passive continental margins [*Gay et al.*, 2003; *Loncke et al.*, 2004; *Naudts et al.*, 2006], indicate that seepage of methane-rich fluids is a common and frequently occurring phenomenon along many continental margins. The combination of large-scale mapping of fluid seeps with studies revealing quantitative aspects of fluid flow is a groundbreaking approach to constraining fluxes at a regional scale.

Acknowledgments

[48] We are indebted to the masters and crews on board the research vessels *Sonne* and *Meteor*. We thank Jens Schneider and Dirk Schwertfeger for their contribution to the seep inventory. The manuscript greatly improved through the action of the associate editor Eli Silver as well as Brian G. McAdoo and an anonymous reviewer. This publication is contribution 153 of the Sonderforschungsbereich 574 "Volatiles and Fluids in Subduction Zones" at Kiel University. In addition, funding was given to Heiko Sahling as part of the DFG-Research Center "Ocean Margins" of the University of Bremen (MARUM 0571).

References

Barckhausen, U., C. R. Ranero, R. von Huene, S. C. Cande, and H.A. Roeser (2001),Revised tectonic boundaries in the Cocos Plate off Costa Rica: Implications for the segmentation of the convergent margin and for plate tectonic models, *J. Geophys. Res.*, *106*(B9), 19,207–19,220, doi:10.1029/2001JB000238.

Bialas, J., E. Flüh, and G. Bohrmann (1999),*Cruise Report SO 144/1&2, PAGANINI, GEOMAR Rep*. 94, GEOMAR, Kiel, Germany.

Bohrmann, G., et al. (2002), Widespread fluid expulsion along the seafloor of the Costa Rica convergent margin, *Terra Nova*, *14*, 69–79, doi:10.1046/j.1365-3121.2002.00400.x.

Bürk, D. (2007), Geoacoustic investigations of cold vents and sedimentary processes at the active continental margin offshore Nicaragua, dissertation thesis, 163 pp., Christian-Albrechts-Universität, Kiel, Germany.

Chan, L.-H., and M. Kastner (2000),Lithium isotopic composition of pore fluids and sediments in the Costa Rica subduction zone: Implications for fluid processes and sediment contribution to the arc volcanoes, *Earth Planet. Sci. Lett.*, *183*, 275–290, doi:10.1016/S0012-821X(00)00275-2.

Clift, P., and P. Vannucchi (2004), Controls on tectonic accretion versus erosion in subduction zones: Implications for the origin and recycling of the continental crust, *Rev. Geophys.*, *42*, RG2001, doi:10.1029/2003RG000127.

De Beer, D., E. Sauter, H. Niemann, N. Kaul, J.-P. Foucher, U. Witte, M. Schlüter, and A. Boetius (2006), In situ fluxes and zonation of microbial activity in surface sediments of the Håkon Mosby Mud Volcano, *Limnol. Oceanogr.*, *51*, 1315–1331.

Fekete, N. (2006), Dewatering through mud mounds on the continental fore-arc of Costa Rica, dissertation thesis, 161 pp., Christian-Albrechts-Universität, Kiel, Germany.

Flüh, E., E. Soeding, E. Suess (2004), *RV SONNE Cruise Report SO173/1, 173/3 and 173/4*, 492 pp., GEOMAR, Kiel, Germany.

Gay, A., M. Lopez, P. Cochonat, N. Sultan, E. Cauquil, F. Brigaud (2003), Sinuous pockmark belt as indicator of a shallow buried turbiditic channel on the lower slope of the Congo Basin, West African Margin, in *Subsurface Sediment Mobilization*, edited by P. Van Rensbergen et al., *Geol. Soc. Spec. Publ.*, *216*, 173–189.

Grevemeyer, I., et al. (2004), Fluid flow through active mud dome Mound Culebra offshore Nicoya Peninsula, Costa Rica: Evidence from heat flow surveying, *Mar. Geol.*, *207*, 145–157, doi:10.1016/j.margeo.2004.04.002.

Han, X., E. Suess, H. Sahling, and K. Wallmann (2004), Fluid venting activity on the Costa Rica Margin: New results from authigenic carbonates, *Int. J. Earth Sci.*, *93*, 596–611, doi:10.1007/s00531-00004-00402-y.

Henry, P., et al. (1996), Fluid flow in and around a mud volcano field seaward of the Barbados accretionary wedge: Results from Manon cruise, *J. Geophys. Res.*, *101*, 20,297–20,323, doi:10.1029/96JB00953.

Hensen, C., and K. Wallmann (2005),Methane formation at Costa Rica continental margin—Constraints for gas hydrate inventories and cross-décollement fluid flow, *Earth Planet. Sci. Lett.*, *236*, 41–60, doi:10.1016/jepsl.2005.06.007.

Hensen, C., K. Wallmann, M. Schmidt, C. R. Ranero, and E. Suess (2004), Fluid expulsion related to mud extrusions off

Costa Rica—A window to the suducting slab, *Geology*, *32*, 201–204, doi:10.1130/G20119.1.

Hühnerbach, V., D. G. Masson, G. Bohrmann, J. M. Bull, W. Weinrebe (2005),Deformation and submarine landsliding caused by seamount subduction beneath the Costa Rica continental margin—New insights from high-resolution sidescan sonar data, in *Submarine Slope Systems: Processes and Products*, edited by D. M. Hodgons and S. S. Flint, *Geol. Soc. Spec. Publ.*, *244*, 195–205.

Kahn, L. M., E. A. Silver, D. Orange, R. Kochevar, and B. McAdoo (1996), Surficial evidence of fluid expulsion from the Costa Rica accretionary prism, *Geophys. Res. Lett.*, *23*, 887–890, doi:10.1029/96GL00732.

Kimura, G., E. A. Silver, P. Blum, and the Shipboard Scientific Party Leg 170 (1997), *Proceedings of the Ocean Drilling Program, Initial Reports*, vol. 170, 458 pp., Ocean Drill. Program, College Station, Tex.

Klaucke, I., D. G. Masson, C. J. Petersen, W. Weinrebe, and C. R. Ranero (2008), Multifrequency geoacoustic imaging of fluid escape structures offshore Costa Rica: Implications for the quantification of seep processes, *Geochem. Geophys. Geosyst.*, *9*, Q04010, doi:10.1029/2007GC001708.

Kulm, L. D., et al. (1986), Oregon subduction zone: Venting, fauna, and carbonates, *Science*, *231*, 561–566, PubMed, doi:10.1126/science.231.4738.561.

Le Pichon, X., K. Kobayashi, and K.-N. S. Crew (1992),Fluid venting activity within the Eastern Nankai Trough accretionary wedge: A summary of the 1989 Kaiko-Nankai results, *Earth Planet. Sci. Lett.*, *109*, 303–318, doi:10.1016/0012-821X(92)90094-C.

Linke, P., K. Wallmann, E. Suess, C. Hensen, and G. Rehder (2005), In situ benthic fluxes from an intermittently active mud volcano at the Costa Rica convergent margin, *Earth Planet. Sci. Lett.*, *235*, 79–95, doi:10.1016/jepsl.2005.03.009.

Loncke, L., J. Mascal, and F. S. Parties (2004),Mud volcanoes, gas chimneys, pockmarks and mounds in the Nile deep-sea fan (Eastern Mediterranean): Geophysical evidences, *Mar. Petrol. Geol.*, *21*, 669–689, doi:10.1016/j.marpetgeo.2004.02.004.

Mau, S., H. Sahling, G. Rehder, E. Suess, P. Linke, and E. Soeding (2006), Estimates of methane output from mud extrusions at the erosive convergent margin off Costa Rica, *Mar. Geol.*, *225*, 129–144, doi:10.1016/j.margeo.2005.09.007.

Mau, S., G. Rehder, I. G. Arroyo, J. Gossler, and E. Suess (2007), Indications of a link between seismotectonics and CH4 release from seeps off Costa Rica, *Geochem. Geophys. Geosyst.*, *8*, Q04003, doi:10.1029/2006GC001326.

McAdoo, B. G., D. L. Orange, E. A. Silver, K. McIntosh, L. Abbott, J. Galewsky, L. Kahn, and M. Protti (1996), Seafloor structural observations, Costa Rica accretionary prism, *Geophys. Res. Lett.*, *23*, 883–886, doi:10.1029/96GL00731.

McIntosh, K. D., and E. A. Silver (1996),Using 3D Seismic reflection data to find fluid seeps from the Costa Rica accretionary prism, *Geophys. Res. Lett.*, *23*, 895–898, doi:10.1029/95GL02010.

McMullin, E., S. Hourdez, S. W. Schaeffer, and C. R. Fisher (2003), Phylogeny and biogeography of deep sea vestimentiferan tubeworms and their bacterial symbionts, *Symbiosis*, *34*, 1–41.

Moerz, T., et al. (2005), Styles and productivity of mud diapirism along the Middle American Margin—Part II: Mound Culebra, Mounds 11 and 12, in *Mud Volcanoes, Geodynamics and Seismicity* edited by G. Martinelli and B. Panahi, 49–76 pp., Springer, New York.

Morris, J. D., and H. W. Villinger (2006),Leg 205 synthesis: Subduction fluxes and fluid flow across the Costa Rica convergent margin, *Proc. Ocean Drill. Program Sci. Results*, *205*, 1–54, doi:10.2973/odp.proc.sr.2205.2201.2006.

Murton, B. J., I. P. Rouse, N. W. Millard, and C. G. Flewellen (1992), Deep-towed instrument explores ocean floor, *Eos Trans. AGU*, *73*, 225–228, doi:10.1029/91EO00184.

Naudts, L., J. Greinert, Y. Artemov, P. Staelens, J. Poort, P. Van Rensbergen, and M. De Batist (2006), Geological and morphological setting of 2778 methane seeps in the Dnepr pleodelta, northwestern Black Sea, *Mar. Geol.*, *227*, 177–199, doi:10.1016/j.margeo.2005.10.005.

Ranero, C. R., and R. von Huene (2000), Subduction erosion along the Middle America convergent margin, *Nature*, *404*, 748–752, doi:10.1038/35008046.

Ranero, C. R., R. von Huene, E. Flueh, M. Duarte, and D. Baca (2000), A cross section of the forearc Sandino Basin, Pacific Margin of Nicaragua, *Tectonics*, *19*, 335–357, doi:10.1029/1999TC900045.

Ranero, C. R., J. P. Morgan, K. McIntosh, and C. Reichert (2003), Bending-related faulting and mantle serpentinization at the Middle America trench, *Nature*, *425*, 367–373, doi:10.1038/nature01961.

Ranero, C. R., I. Grevemeyer, H. Sahling, U. Barckhausen, C. Hensen, K. Wallmann, W. Weinrebe, P. Vannucchi, R. von Huene, and K. McIntosh (2008), Hydrogeological system of erosional convergent margins and its influence on tectonics and interplate seismogenesis, *Geochem. Geophys. Geosyst.*, *9*, Q03S04, doi:10.1029/2007GC001679.

Saffer, D. M., E. A. Silver, A. T. Fisher, H. Tobin, and K. Moran (2000), Inferred pore pressure at the Costa Rica subduction zone: Implications for dewatering processes, *Earth Planet. Sci. Lett.*, *177*, 193–207, doi:10.1016/S0012-821X(00)00048-0.

Schmidt, M., C. Hensen, T. Mörz, C. Müller, I. Grevemeyer, K. Wallmann, S. Mau, and N. Kaul (2005), Methane hydrate accumulation in "Mound 11" mud volcano, Costa Rica forearc, *Mar. Geol.*, *216*, 83–100, doi:10.1016/j.margeo.2005.01.001.

Screaton, E. J., and D. M. Saffer (2005),Fluid expulsion and overpressure development during initial subduction at the Costa Rica convergent margin, *Earth Planet. Sci. Lett.*, *233*, 361–374, doi:10.1016/jepsl.2005.02.017.

Shipley, T. H., and G. F. Moore (1986),Sediment accretion, subduction, and dewatering at the base of the trench slope off Costa Rica: A seismic reflection view of the décollement, *J. Geophys. Res.*, *91*, 2019–2028, doi:10.1029/JB091iB02p02019.

Shipley, T. H., P. L. Stoffa, and D. F. Dean (1990), Underthrust sediments, fluid migration paths, and mud volcanoes associated with the accretionary wedge off Costa Rica: Middle America Trench, *J. Geophys. Res.*, *95*, 8743–8752, doi:10.1029/JB095iB06p08743.

Shipley, T. H., K. D. McIntosh, E. A. Silver, and P. L. Stoffa (1992), Three-dimensional seismic imaging of the Costa Rica accretionary prism: Structural diversity in a small volume of the lower slope, *J. Geophys. Res.*, *97*, 4439–4459, doi:10.1029/91JB02999.

Sibuet, M., and K. Olu (1998), Biogeography, biodiversity and fluid dependence of deep-sea cold-seep communities at active and passive margins, *Deep Sea Res., Part II*, *45*, 517–567, doi:10.1016/S0967-0645(97)00074-X.

Silver, E. A., M. Kastner, A. Fisher, J. Morris, K. McIntosh, and D. Saffer (2000), Fluid flow paths in the Middle American Trench and Costa Rica margin, *Geology*, *28*, 679–682, doi:10.1130/0091-7613(2000)28<679:FFPITM>2.0.CO;2.

Söding, E., K. Wallmann, E. Suess, and E. Flüh (2002), *RV METEOR Cruise Report M54/2 and 54/3*, 366 pp., GEOMAR, Kiel, Germany.

Talukder, A. R., J. Bialas, D. Klaeschen, D. Buerk, W. Brueckmann, T. Reston, and M. Breitzke (2007), High-resolution, deep tow, multichannel seismic and sidescan sonar survey of the submarine mounds and associated BSR off Nicaragua Pacific margin, *Mar. Geol.*, *241*, 33–43, doi:10.1016/j.margeo.2007.03.002.

Vannucchi, P., C. R. Ranero, S. Galeotti, S. M. Straub, and D. W. Scholl (2003), Fast rates of subduction erosion along the Costa Rica Pacific margin: Implications for nonsteady rates of crustal recycling at subduction zones, *J. Geophys. Res.*, *108*(B11), 2511, doi:10.1029/2002JB002207.

von Huene, R., and D. W. Scholl (1991), Observations at convergent margins concerning sediment subduction, subduction erosion, and the growth of continental crust, *Rev. Geophys.*, *29*, 279–316, doi:10.1029/91RG00969.

von Huene, R., C. R. Ranero, and W. Weinrebe (2000), Quaternary convergent margin tectonics of Costa Rica, segmentation of the Cocos Plate, and Central American volcanism, *Tectonics*, *19*, 314–334, doi:10.1029/1999TC001143.

von Huene, R., C. R. Ranero, and P. Vannucchi (2004a), Generic model of subduction erosion, *Geology*, *32*, 913–916, doi:10.1130/G20563.1.

von Huene, R., C. R. Ranero, and P. Watts (2004b), Tsunamigenic slope failure along the Middle American Trench in two tectonic settings, *Mar. Geol.*, *203*, 303–317, doi:10.1016/S0025-3227(03)00312-8.

von Rad, U., et al. (2000), Gas and fluid venting at the Makran accretionary wedge off Pakistan, *Geo Mar. Lett.*, *20*, 10–19, doi:10.1007/s003670000033.

Wallmann, K., M. Drews, G. Aloisi, and G. Bohrmann (2006), Methane discharge into the Black Sea and the global ocean via fluid flow through submarine mud volcanoes, *Earth Planet. Sci. Lett.*, *248*, 544–560, doi:10.1016/jepsl.2006.06.026.

Weinrebe, W., and E. Flüh (2002), *R/V SONNE Cruise Report SO 163*, 534 pp., GEOMAR, Kiel, Germany.

Werner, R., K. Hoernle, P. van der Bogaard, C. R. Ranero, R. von Huene, and D. Korich (1999), A drowned 14 Ma old Galápagos Archipelago off the coast of Costa Rica: Implications for evolutionary and plate tectonic models, *Geology*, *27*, 449–452.

Westbrook, G. K., and T. J. Reston (2002), The accretionary complex of the Mediterranean Ridge: Tectonics, fluid flow and the formation of brine lakes—An introduction to the special issue of Marine Geology, *Mar. Geol.*, *186*, 1–8, doi:10.1016/S0025-3227(02)00169-X.

Zuleger, E., J. M. Gieskes, and C.-F. You (1996), Interstitial water chemistry of sediments of the Costa Rica accretionary complex off the Nicoya Peninsula, *Geophys. Res. Lett.*, *23*, 899–902, doi:10.1029/96GL00386.